NBSIR 87-3066

DEVELOPMENT OF STANDARDS FOR SUPERCONDUCTORS

Interim Report
January–December 1985

L.F. Goodrich, S.L. Bray, W.P. Dube, E.S. Pittman, A.F. Clark
Electromagnetic Technology Division
Center for Electronics and Electrical Engineering
National Engineering Laboratory
National Bureau of Standards
Boulder, Colorado 80303-3328

APRIL 1987

NBSIR 87-3066

DEVELOPMENT OF STANDARDS FOR SUPERCONDUCTORS

Interim Report
January–December 1985

L.F. Goodrich, S.L. Bray, W.P. Dube, E.S. Pittman, A.F. Clark
Electromagnetic Technology Division
Center for Electronics and Electrical Engineering
National Engineering Laboratory
National Bureau of Standards
Boulder, Colorado 80303-3328

APRIL 1987

U.S. DEPARTMENT OF COMMERCE, Malcolm Baldrige, Secretary

NATIONAL BUREAU OF STANDARDS, Ernest Ambler, Director

The ultimate goal of this research program is to develop fundamental understanding, a technology base, consensual standard definitions, consensual standards of measure, and standard reference materials for superconductor parametric measurements. The program areas and elements are based on the intersection of our expertise and capabilities with recommendations from the research community and sponsors. The emphasis and priorities are flexible and the program responds to new problems as they arise.

The key parameters in the commerce of superconductors need standard definitions and standards of measure. These parameters include critical current, stability, strain dependence, transient loss, critical magnetic field, and critical temperature. The standards are voluntary, and developed by users and producers; we hope thereby to achieve an overall balance of simplicity and accuracy. The fundamental understanding acquired during the standardization will be disseminated to the community through open literature publications. Where appropriate, Standard Reference Materials (SRM's) will be developed to promote more-uniform measurements and to serve as a means for interlaboratory comparisons that will further advance the consensus and evolution of standard test methods. This research program is focused on three areas: critical current, stability, and SRM's. The original program direction was to continue with a large part of the research on large conductor critical current and to begin increasing emphasis on stability and eventually another critical current SRM. Because of the number of problems and interest in large conductor critical current, and a small reduction in available funds and staff, the emphasis has remained on critical current measurements.

A key parameter in the technology of superconducting wire is critical current; at present there is no standard test method for large conductor critical current (greater than 600 A). The measurement problems and parameters must be understood before a new high-current consensual standard test method can be developed. Such a standard will increase measurement accuracy, reduce test time, and lower conductor cost.

Superconductor stability is an important parameter in the technology of large magnets. It ranks in importance near critical current as a design parameter. A few experiments have tried to measure stability directly, and several heat transfer tests could be used to acquire data for calculating its value. If a meaningful and practical test method for stability could be developed, it would reduce much of the uncertainty and conservatism currently used in the design of large superconducting magnets, resulting in both savings in cost and increased magnet performance.

An SRM provides a means for checking the overall accuracy of the complex systems used to measure superconductor parameters. Traceability of standards is important to the evaluation of superconductor technology. SRM's can also provide interlaboratory comparisons and promote fair competition among suppliers.

An effort was made to avoid the identification of commercial products by the manufacturer's name, but in some cases these products might be indirectly identified by their particular properties. In no instance does this imply endorsement by the National Bureau of Standards, nor does it imply that the particular equipment is necessarily the best or worst available for this purpose.

CONTENTS

DEVELOPMENT OF STANDARDS FOR SUPERCONDUCTORS

Interim Report
January - December 1985

L. F. Goodrich, S. L. Bray, W. P. Dube, E. S. Pittman, and A. F. Clark

Electromagnetic Technology Division
Center for Electronics and Electrical Engineering
National Engineering Laboratory
National Bureau of Standards
Boulder, Colorado 80303

A cooperative program with the Department of Energy, the National Bureau of Standards, and private industry is in progress to develop standard measurement practices for use in large scale applications of superconductivity. The goal is the adoption of voluntary standards for the critical parameters and other characterizations of practical superconductors. Progress for the period January through December 1985 is reported. The major effort was the measurement of large conductor critical current. Other work reported here includes stability and a discussion of possible future Standard Reference Materials.

Key words: angle; aspect ratio; cable; critical current; critical parameters; measurement; standards; superconductor

INTRODUCTION

This report covers the period January 1984 through December 1985. Most of 1984 was devoted to completing the critical current measurements of the small conductor Standard Reference Material (SRM). The special publication on the SRM [1] serves as the report for 1984. The sections of this report cover topics other than the SRM and include a few efforts from 1984. Two recent publications are included as Appendices A and B [2,3]. A complete list of the more than 35 publications resulting from this project is given as Appendix C.

This report covers the measurement of large conductor critical current and the parameters that affect stability. Experimental concerns, measurement checks, and results are presented. This report deals mostly with large conductor critical current. Stability and the next SRM will be phased in during the following years of this program.

CRITICAL CURRENT

The differences between critical current measurements on large and small conductors are that some previously negligible parameters become significant and other new parameters are introduced. The expense of increasing high magnetic field volume restricts the scale-up of magnets used in critical current testing, which causes the effects of current injection, current transfer, and bending strain to become more significant for large conductor measurements. Our measurements have not indicated any change in the character of current transfer in large conductors. The self-field of the sample and the field of the current return path become more significant at the higher currents. The increased Lorentz force and torque on the sample and magnet supports can cause additional motion-induced noise and systematic steady state voltage shifts. Ripple in the current supply becomes more significant at the higher current levels because filtering is more difficult. Ripple also affects the sample voltmeter, which has to operate with a very noisy input and have high common mode rejection. New measurement problems and parameters occur in cable conductors. The inherent variation of critical current along the length of a strand will cause intrinsic current transfer and complications in voltage tap placement and interpretation. These inherent variations can be due to changes in conductor cross-sectional area, field angle, conductor aspect ratio, strain, self-field, and possible degradation of the super-conducting properties.

All of the large conductor measurements to date have been conducted with a 10 T radial access magnet. Therefore, some of the observations reported here are particular to that geometry. The small bore diameter (3.8 cm) of our 9 to 10 T solenoid magnet did not lend itself to large conductor testing. However the radial access magnet allowed for changing the orientation of the sample relative to the background magnet which is very useful for large conductor and cable measurements. We have started procurement of a 12 T solenoid with a 12.7 cm diameter. This large bore solenoid will allow for testing of longer and higher current samples.

The body of this section of the report is devoted to a number of new experimental concerns that developed with critical current measurements on large conductors. Results of these measurements are given in Appendix A.

These new concerns affect the critical current measurements and thus limit the precision and accuracy of the measurement. To proceed it is necessary to recognize, understand, and attempt to reduce these effects. The progress that has been made toward this end is detailed below.

Present Capabilities

During this period, we constructed a sample cryostat with 3000 A capacity and made our first measurements in this current range. We reduced the amount of 60 Hz harmonic ripple in our 3000 A power supply. We also increased the capacity of our low-noise battery power supply from 600 to over 900 A and reduced the noise level from 0.5 A peak-to-peak to 0.01 A peak-to-peak. We have also further automated data acquisition and can now measure three voltage tap pairs at once. This reduced operator fatigue and increased the quantity of the data. The changing of voltage taps, magnetic field, and angle are still done manually. We had developed automatic data analysis when making the first SRM. Our data acquisition programs were modified to handle current transfer voltage, voltage filtering, and the time lag of some volt-meters in order to be used in large conductor data analysis.

Short Range Variations

Here, we discuss the large variations in critical current that have been observed over a very short length of wire. The first report of this is reproduced here as Appendix A. Refer to the bottom of the fourth page through the top of the sixth page and figures 5, 6, and 7 of Appendix A. This type of variation is of fundamental and practical importance, especially in the making of an SRM. These effects may also be present in cable conductors due to turkshead compaction. To a much smaller extent, short range variations were present in the first SRM, which had a round cross section, although it is not known if these short range variations occurred due to the same mechanism.

These variations in critical current seem to be periodic and associated with changes in filament deformation. The variation in filament deformation observed here appears to be different from sausaging [4] in that here change in deformation occurs collectively (most of the filaments together) rather than randomly as in sausaging. Also, the extreme deformation was a flattened filament, rather than a necked filament as in sausaging.

The cause of this periodic variation in filament shape, critical current, and aspect ratio was the most likely combination of filament twist and hexagonal filament array [5]. This apparent mechanical instability can be envisioned by considering that the turkshead will try to remove the filament twist and the torque will build up in front of the turkshead until the aligned filaments slip through with extreme deformation.

A key to reducing this effect may be the center copper island [6] or the local copper-to-superconductor ratio. Compare figures 5 and 7 in Appendix A. The change in shape of the copper island in figure 7 indicates that it may be playing an important role in reducing the extreme filament deformation.

Persistent Currents

Persistent currents among the sample current return wires caused a time dependent, partial shielding of the sample from the applied magnetic field. Four return wires were used on the radial-access-magnet cryostat for a number of reasons: higher current capacity, reduced net torque on the sample cryostat, and reduced effect of the magnetic field of the return path on the sample. The four return wires were soldered together at each end (onto the sample and onto the bus bar). This resulted in a relatively long decay time constant of about 25 seconds. A delay of several time constants is required between each measurement after the cryostat is rotated or the background magnetic field is changed. This slowed down the measurement process and also resulted in some points being taken too soon after a change, which compromised the entire data set.

A solution was to add a small resistance (brass shims, approximately 50 nΩ) to each return wire between the wire and the bus bar. This reduced the decay time constant from 25 s to 5 s. The added heating at this location was not a problem. An effort was made to keep the solder from bridging across the brass shims, since they were located in the stray magnetic field and the solder would be superconducting for some sample magnetic fields. These resistors also helped ensure that the current was shared more evenly among the return wires.

Two pick-up coils were placed on the sample holder to measure the change in the magnetic field applied to the sample. These two coils were oriented about 90 deg. apart in order to measure both components of the magnetic field. These coils verified the estimated decay time constants and the sample motion problems.

A further observation was that these return wires can shield some of the time-changing magnetic flux during a fast ramp (large dI/dt) of the sample current. The shielding effect seems only to be significant when the sample is not straight, such as a strand extracted from a cable. In such cases errors may occur in the determination of mutual inductance of the voltage taps which can result in small errors in the critical current determination. Other sources that result in errors in the determination of mutual inductance are self inductance of the sample, shielding currents in the copper matrix, and sample motion as the Lorentz force is increasing. Although these other sources are present, the return wires are believed to be the dominant source.

Using multiple return wires has some disadvantages, but the advantages outweigh them. When doing fundamental studies, it was better not to complicate the measurements with extra magnetic field corrections. The reduction in the net force and torque on the sample holder also helped lower the voltage noise.

Motion

One of the identified experimental problems was motion of the sample and leads. Voltage noise as large as several microvolts can be introduced by slight motion of the sample holder. This motion is caused by the increasing Lorentz force as the current is increased during data acquisiton. The net force on the sample cryostat is not zero if the current return path does not

traverse exactly the same magnetic field profile as the sample path. If the current sharing among the four return wires is not perfect there will also be a net torque on the sample cryostat. Additionally, stray Lorentz forces and mechanical vibrations can cause relative motion of the magnet and sample. Motion of the leads between the top of the cryostat and the voltmeter input connections will cause voltage due to the stray magnetic field.

The noise was reduced to less than the intrinsic voltmeter noise with the addition of a band brake device that was mounted on the top of the magnet. This brake could be tightened around the sample cryostat with a room temperature screw actuator, thus restricting the relative motion between the magnet and sample.

The band brake device consisted of a power screw, band, stop, and stainless steel tube. The stainless steel tube goes from the top of the cryostat to the top of the magnet. The stop consisted of two aluminum angles fastened to the top of the magnet so that they each were tangent to the edge of a G-11 flange on the sample cryostat. The band was a stainless steel cable that loops around the edge of the G-11 flange on the sample cryostat. Springs were used to hold the cable away from the G-11 flange when not under tension to allow the sample cryostat to be inserted. The power screw assembly was also mounted on the top of the magnet and it translated a small torque on a stainless steel tube into a large tensional force in a cable. This force holds the cryostat against the aluminum angles and reduces the relative motion between the cryostat and magnet.

Pressure Control

The measurement of the temperature dependence of critical current is best conducted in a constant temperature bath of liquid helium because of the high current involved and for better sample stability. This measurement needs to be done when making an SRM, direct comparisons with other laboratories, and fundamental studies. Since this testing site has a relatively low ambient pressure (liquid helium equilibrium temperature about 4.0 K), most of these measurements are made above ambient pressure. The easiest way to keep a bath at constant temperature is to use an automatic pressure controller to control the vapor pressure. One of the unusual aspects of pressure control during the critical current measurement is that the gas flow can change by 20 to 30 percent caused by the increased boil-off during the data acquisition or while ramping the magnet.

Several types of controllers have been used. A good reference is a book on low temperature laboratory techniques by Rose-Innes [7]. In the past, we have used a commercial Cartesian manostat but it was not able to control the Dewar pressure during large conductor testing. It could not handle the high boil-off rate, even with 60 to 80 percent of the flow bypassing the controller. It was also difficult to set the reference pressure. Therefore a diaphragm type manostat [8] was constructed. The design was similar to the original reference [9]. The key changes were: a plastic diaphragm, a diaphragm limiting plate with holes to reduce oscillation, a large port with holes to allow for more gradual opening, and a large reference pressure chamber so that this pressure does not change as much with flow variation.

Increasing the impedance in the exhaust port, decreased the pressure at the intake port as the flow increased. This was because as the difference in the port pressures decreased, less inlet pressure was required to lift the diaphragm off the exhaust port. On the other hand, if the exhaust impedance was set too high, the system pressure would run away. An empirical setting of the exhaust pressure that allowed a sufficient range of flow rates was determined. This inverse relationship between inlet pressure and flow rate partially compensated for the increase in pressure drop across the vapor cooled leads with increased gas flow, thus, stabilizing the dewar pressure with respect to gas flow rate. Pressure control to ±133 Pa (±1 mm Hg, ±1.4 mK) was achieved with a helium boil-off rate of 8 liters of liquid per hour.

Improvements to 3000 A Supply

Our high-current power supply is a unit manufactured originally as a 3000 A electroplating supply. The manufacturer supplied a single-section filter. As received, its noise level was substantial. The noise consisted of two components; spike voltages that exceeded 160 V peak, and 3-phase current ripple on the output of 50 A RMS. Also, the output was coupled to ground through a fairly low resistance. The effect of this was a ground loop that resulted in systematic measurement errors.

The spike voltages resulted from rapid switching of the transformer primary windings through silicon-controlled rectifiers (SCR's). High voltage 0.2 mF capacitors were connected across the SCR's in order to reduce the switching speed and, thus, reduce the spike voltages. This resulted in a reduction in the spike voltages by several orders of magnitude. Reducing the switching speed of the SCR's increases their power dissipation. Consequently, reduction of the switching speed is limited by their ability to dissipate power without damage.

The current ripple presented a much more difficult problem. The filter was cleaned of varnish at all contact points. To reduce the series resistance of the 0.5 F capacitor bank, originally connected with 10 gauge wire, it was rewired with heavy bus bars. The net result was a reduction in current ripple of the output by more than a factor of 2.

The excessive conductance to ground was traced to leakage through the diode rectifier water cooling system. This was remedied by insulating the cooling system at all points where it contacted the chassis. This resulted in leakage current having to travel the full length of the cooling pipes which, in turn, greatly reduced the conductance from the dc output to ground.

Finally, the cooling system, as set up, was thermostatically controlled. The thermostat sensed the temperature of a heat sink and turned the cooling system on and off with solenoid valves. These electrically noisy valves produced massive bursts of noise which were picked up by the low level measurement equipment. The solution was to replace the thermostat with a temperature-controlled, continually variable flow valve. This valve is a passive nonelectrical device.

The battery powered current supply has been modified in several areas to improve its performance. First, the current output capability of the supply has been increased from 600 A to 900 A. Second, the supply's susceptibility to ground loop problems has been reduced. Third, the current output has been linearized and, fourth, the noise level of the supply has been lowered considerably. This current supply represents the long term evolution of a much simpler design and as such is not an optimal design.

The original design achieved current amplification through a three-stage common collector transistor cascade. The final stage of the amplifier consisted of a parallel combination of two 300 A power transistors. In order to increase the current capability of the supply, the present design's final stage uses six Darlington transistor pairs, each pair consisting of a 25 A and a 300 A power transistor. This modification resulted in an increase of 50 percent in the peak current capability of the supply. Presently, the current capacity of the supply is limited by the internal resistance of the battery cells (two 1350 A√h, 2 V cells) and the limited output capacity of the control circuit.

As noted below in the "Test Method For Low Level Voltage Measurement Systems" section of this report, ground loops are often a source of error when making low level voltage measurements of the type required in superconductor testing. In the case of the battery powered current supply, the input ramp generator is capacitively coupled to ground. Because it is impossible to eliminate all additional grounds in the circuit and the test apparatus, the ramp generator required electrical isolation from the remainder of the supply circuit in order to eliminate the ground loop problem. Consequently, optical couplers and a separate dc power supply were used at the input stage of the supply circuit (a 110 V/15 V supply was used prior to the electrical isolation boundary and 6 V batteries were used after the boundary - see fig. 1). This modification resulted in a considerable reduction of systematic measurement errors.

A major flaw of the original current supply was that its output was nonlinear. Moreover, a linear voltage ramp input (dv/dt=constant) did not result in a linear current ramp output (di/dt=constant). This nonlinear behavior resulted in a variable inductive voltage (due to the di/dt variation) across the sample's voltage taps. For a ramp input, an inductive voltage is impossible to avoid. However, if this voltage is constant, it is easily separated from the desired resistive voltage measurement.

The linearity of the battery current supply was greatly improved through the use of feedback control. Feedback loops were used at two points in the circuit, one on each side of the electrical isolation boundary. In both cases operational amplifers were used as comparators between the reference and feedback signals. Ideally, the first feedback signal would be taken from the same point in the circuit as the input to the second comparator. However, this would defeat the purpose of the optical couplers by creating an electrical coupling between the input and output stages of the circuit. Consequently, it was necessary to employ a second optical coupler connected in series with the first as a source of the feedback signal. Inasmuch as the two optical couplers are not perfectly matched, this feedback signal is not ideal
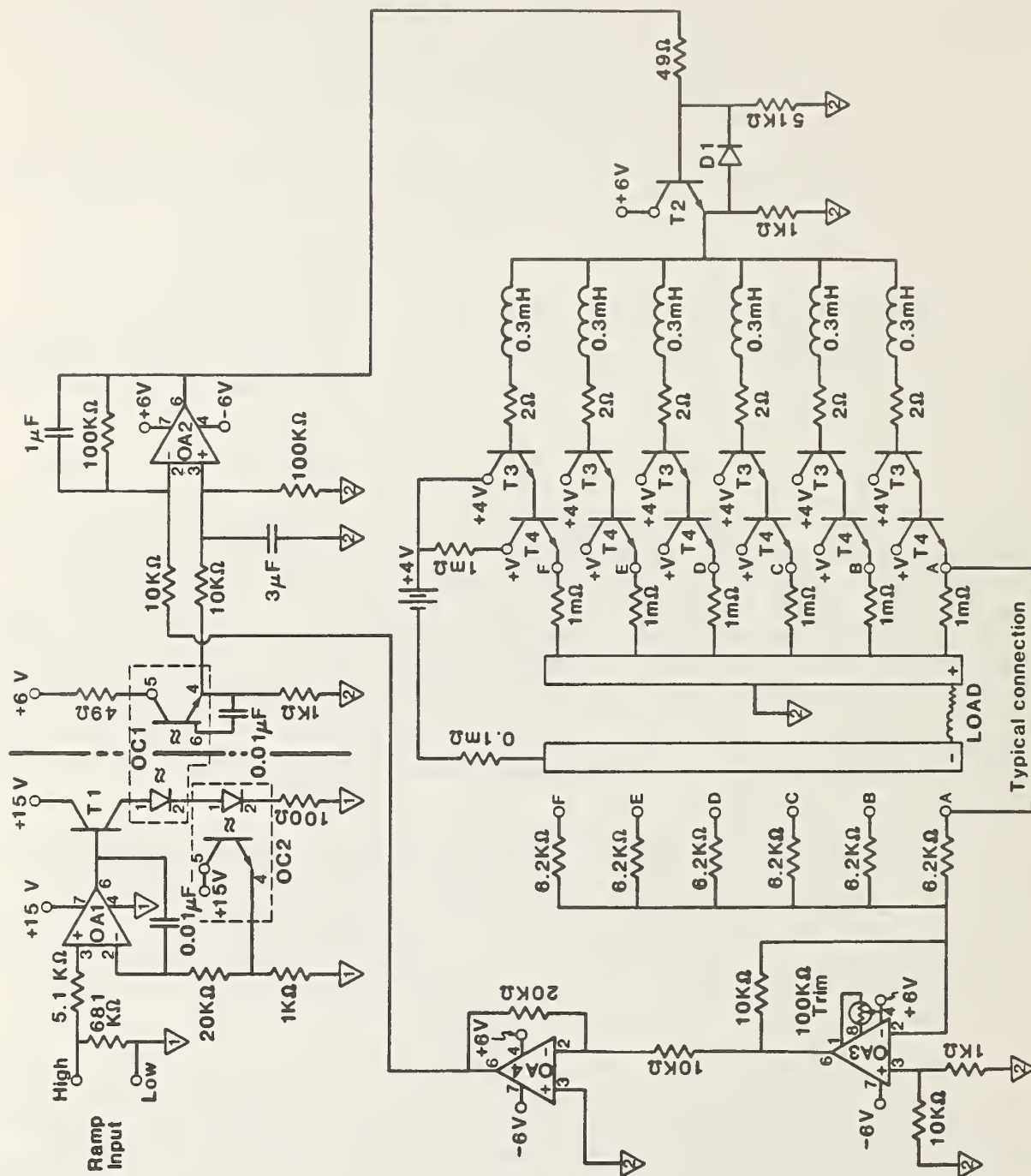
Figure 1. Schematic circuit diagram of battery powered current supply.

8

and may result in some residual nonlinearity. The second feedback signal
originates at the output terminals of the six Darlington pairs. Another
operational amplifier, configured as an inverting summer, combines, inverts
and amplifies these six signals. The resulting signal is then amplified and
inverted by a second operational amplifier in the feedback loop and then
applied to the comparator.

Another source of residual nonlinearity is the limited gain of the
comparators. This limited gain is necessary to avoid oscillation, which is a
common problem with this type of circuit. Similarly, the capacitors in the
feedback loops of the comparators are necessary to reduce AC gain. Also,
there is a tendency toward parasitic oscillation in the Darlington output
stage. This instability has been effectively controlled by the addition of
the 0.3 mH inductors at the Darlington inputs.

Overall, these modifications have resulted in very good linearity over
the required current range and load conditions. Figures 2, 3, and 4 indicate
the relative linearity of the system. These are plots of the output current's
deviation from linearity (ΔI, A) vs. the output current (I, A). The plots
show hysteresis with the lower curve corresponds to increasing current while
the upper curve corresponds to decreasing current. The first plot (fig. 2)
shows the total nonlinearity of the system. The two remaining plots, figures
3 and 4, indicate, respectively, the relative contribution to nonlinearity
made by the electrical isolator (circuitry on input side of isolation
boundary) and that made by the remainder of the system. From these plots it
is evident that the majority of the nonlinearity is due to the electrical
isolator. It is important to note that, although these plots have been scaled
in order to accentuate the deviation from linearity, the percentage deviation
is actually quite small. Moreover, at an output current of 800 A the maximum
deviation from linearity is less than 2.5 percent.

As the current supply design evolved and improved it became desirable to
reduce the level of 60 Hz noise which was present at the output. Several
noise sources were identified; the first of which was the input ramp
generator. The use of a passive filter between the ramp generator and the
supply reduced the input noise; however, a comparable reduction in the output
noise was not realized, indicating the presence of another noise source. An
unused terminal (#6 see fig. 1) on the first optical coupler was suspected of
being a significant noise source. Effective filtration of this noise was
achieved by connecting a capacitor from this terminal to the emitter (terminal
#4) of the optical coupler. As a result, the noise level has been reduced
from 0.12 A to 0.01 A, peak to peak. The residual noise may be due to
additional pickup and incomplete filtering. Although the current supply has
been greatly improved, further modifications and a new application of the
design are currently being investigated. Specificly, several methods for
reducing the nonlinearity of the electrical isolation system have been
proposed and are being tested. Also, the reset time (in the event of a sample
quench the supply must be rapidly reset to zero current) was increased because
of the additional filtering within the control circuit. This longer reset
time is undesirable and a remedy is under development. Finally, a new
application for the battery powered current supply is being tested. This
application involves using the battery supply in parallel with the 3000 A
current supply (see above for information regarding the 3000 A supply) in
order to reduce the amount of current ripple (harmonics of 60 Hz) and increase
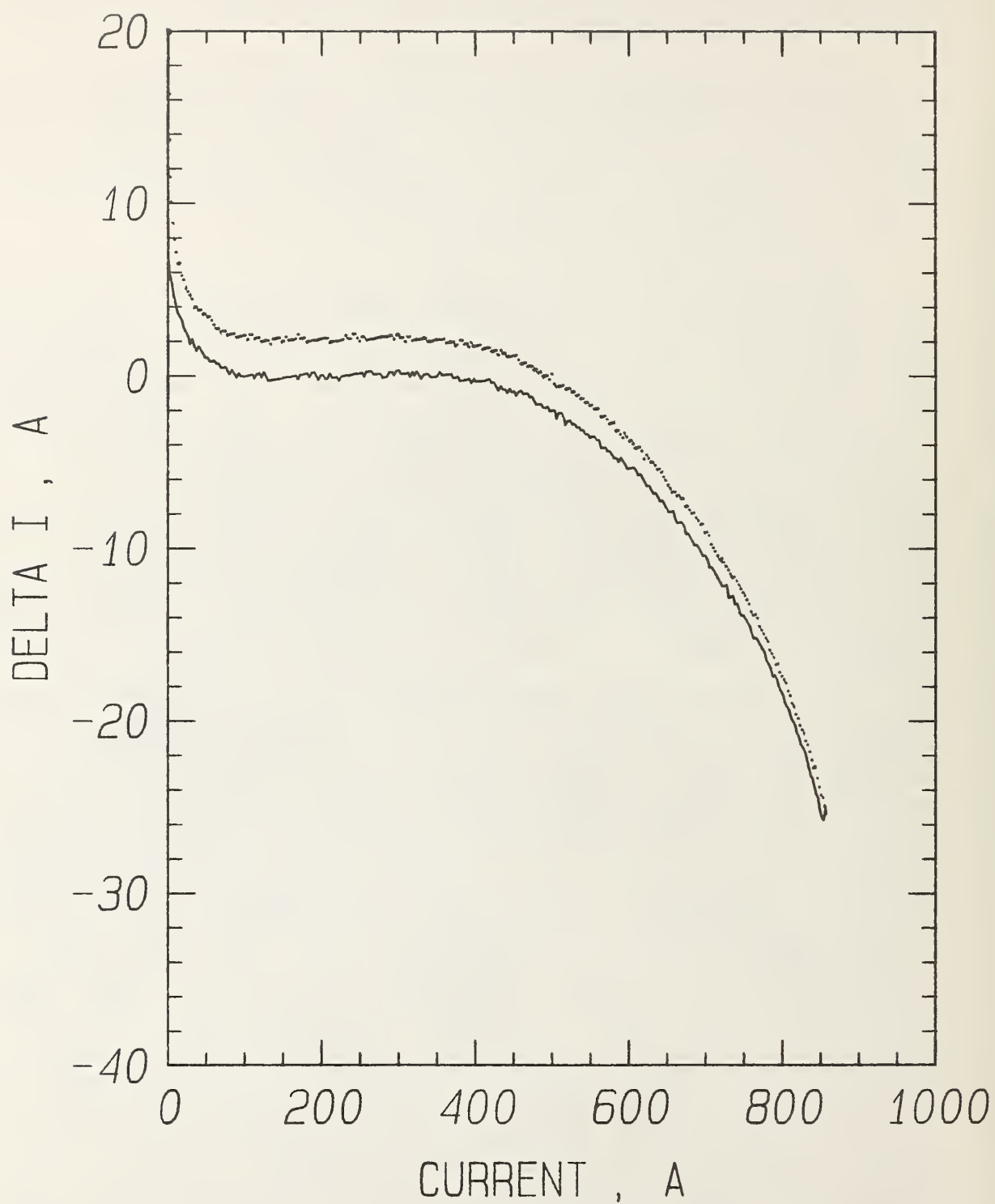
Figure 2. Output currents deviation from linearity versus output current from the entire supply circuit.
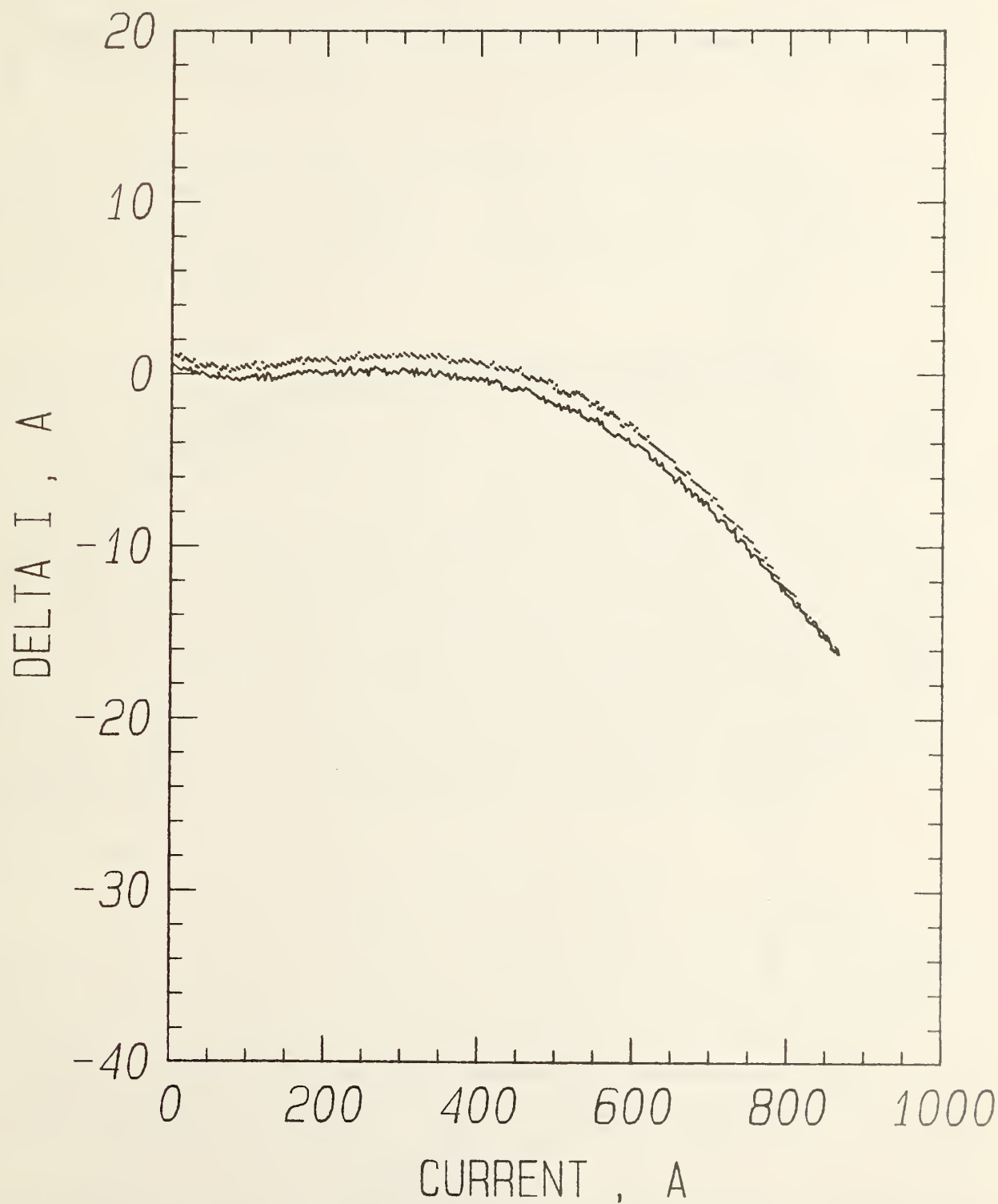
10

Figure 3. Output currents deviation from linearity versus output current from
the circuitry on the input side of the isolation boundary.
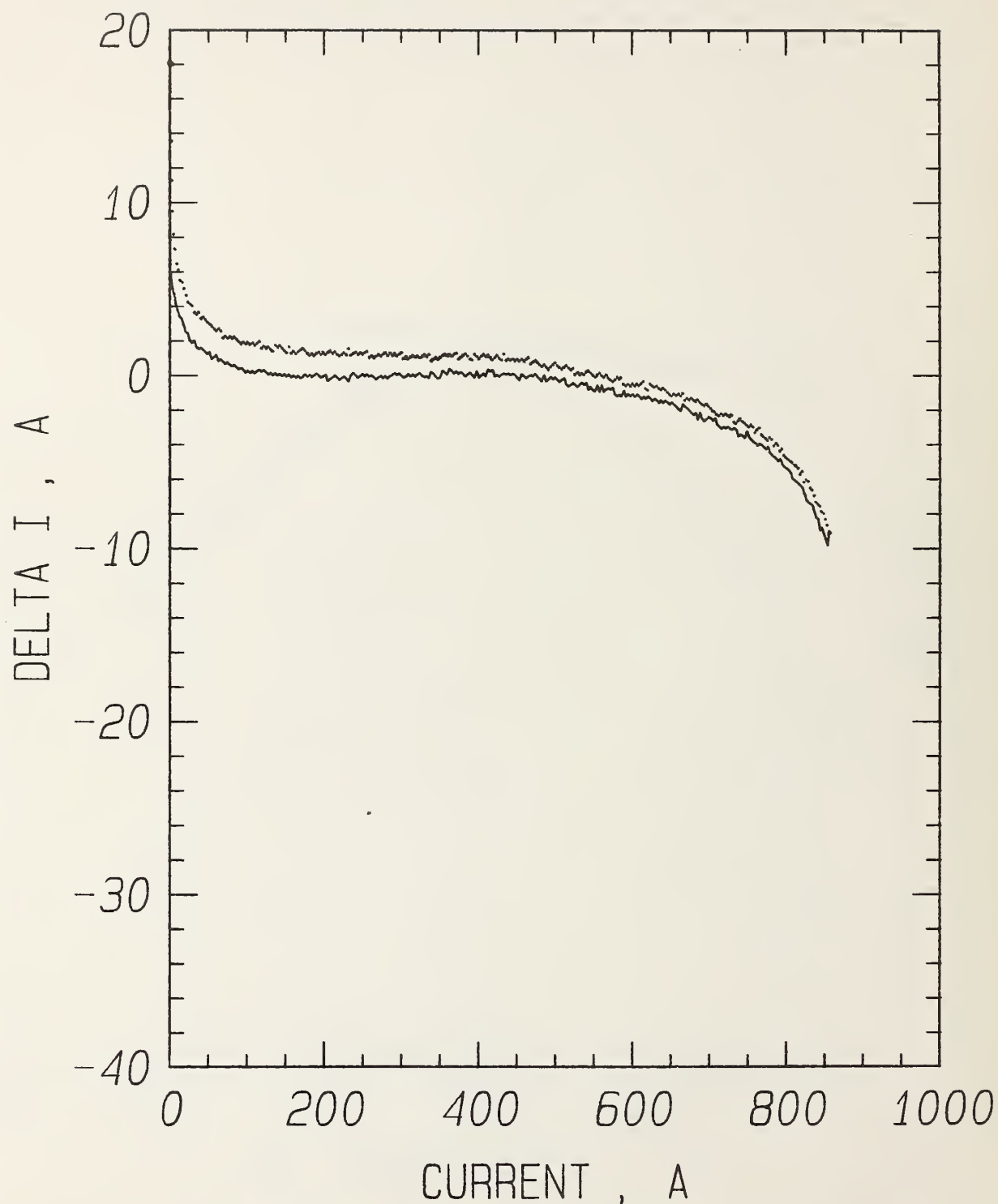
11

Figure 4. Output currents deviation from linearity versus output current from the circuitry on the output side of the isolation boundary.

12

the total output capability of the 3000 A supply. Reducing the current ripple would decrease the voltage noise and uncertainty of the current. Initial feasability tests have been made and the results are promising.

User Notes on Digital Voltmeters

Experience using a digital nanovoltmeter with an amplified analog output has revealed some advantages and some cautions. These properties may or may not be true for all such instruments.

The advantages of digital nanovoltmeters are high noise and common-mode rejection, high voltage gain, and electrical isolation of amplified analog output. This isolation is achieved using optical coupling between the digital and analog systems. This isolation can reduce the risk of ground loops. The high gain is achieved in the digital-to-analog conversion. The anolog output is a continuous signal constructed by connecting adjacent digital points with straight line segments.

Two cautions that should be brought to the user's attention concern time lag and internal digital filtering. The time lag of the analog-to-digital and digital-to-analog converters is about 0.6 and can be accounted for in some computer aided data acquisition systems. To make low level measurements, a lot of filtering and damping are used to make the display steady for visual readings. This can slow the response time to the point where it is not useful for even slow direct current sweeps. Additionally, an internal digital filter is used that switches in and out depending whether the latest reading is significantly different from the average. This is done so that the instrument can respond faster to step functions. This filter can be turned off only over the computer bus and will switch back in on a bus reset or a front panel filter or damping selection. With the filter in, a smooth voltage increase with time will appear as a sawtooth waveform because this filter is coming in and out with time. This is a problem for critical current measurements and can be a problem in precise steady state measurements such as resistivity. In the latter case, the filter can give increased statistical weight to outlying readings. A passive (constant) filter on the amplified signal and/or statistical curve fitting of the waveform is required for precise determinations.

Test Method For Low Level Voltage Measurement Systems

It can be difficult to measure the low voltages that are required in critical current testing. A simple technique to check for voltage measurement problems in a system is described. This technique will provide information on general system integrity, voltage noise, inductive voltage, thermoelectric voltage, and false voltages for a new system or when a system is significantly modified. False voltages can arise from ground loops and common mode voltages. The common-mode rejection ratio (CMRR) is one of the factors that indicates the meter's ability to make true voltage measurements with the presence of common mode voltage. Some of the false voltage could also depend on the design of the voltmeter's input stage.

The test can be done at room temperature without the sample cryostat and vapor cooled leads. A dummy sample is a copper block that has a cross-sectional area that can easily carry several times the peak current. Estimate

13

the resistance per unit length and calculate what separation would provide a typical voltage. Put two voltage taps with this separation near the center of the dummy sample. The voltage taps can be staggered so that they are almost at the same potential. The desired separation is one that allows for the same voltage and current ranges as in the critical-current measurement. In this case, place the dummy sample directly across the ends of the sample current supply bus bar. If it is desired to use the sample voltage leads, then place the dummy sample (as a shunt) across the vapor cooled leads and sample.

The first check is a finite resistance measurement where the resistance between two voltage taps is measured by sweeping the current from zero to full value and then back down to zero again. The measured resistance can be checked with the calculated value. This serves as a check for the system, and results can be compared to previous or future measurements and other voltmeters. If the dummy sample is not very long compared to its diameter, the measured resistance can change because of variation in current injection at the current contacts. An effort can be made to have uniform and/or consistent current injection. It may be useful to have two pairs of voltage taps, one pair with the largest separation allowed by the voltage and current scales and the other closer to the lower limits of the system. The precision and repeatability of the measurement are easier to check with the more widely spaced voltage taps. The voltage noise, inductive voltage and changes in thermoelectric voltage will become more significant for the closer pair.

Three voltmeters (A, B, and C) were tested on a dummy sample using two sample current supplies (battery and 3000 A SCR). These two supplies are described in separate sections of this report. Meter A, a digital nano-voltmeter with an amplified analog output, is described in the section entitled User Notes on Digital Voltmeters. Meter B is an analog nanovoltmeter with amplified output. Meter C is a digital microvoltmeter that has a low-noise, analog preamplifier (gain of 100) with an external output available.

Examples of this test are shown in figures 5, 6, 7, and 8. All of these figures show voltage versus current for increasing (lower curve) and decreasing current (upper curve). Figure 5 was taken using Meter A and a 3000 A power supply. Figures 6, 7, and 8 were taken respectively using Meters A, B, and C with a battery power supply. The measured resistance was about 1.5 nΩ with some variation due to changes in current injection at the current contacts.

The next test, a zero resistance test, will check for ground loop and common mode voltage problems. This test is the same as the first except the voltmeter input leads are both connected to the same tap on the dummy sample. This simulates an ideal superconductor - no resistive voltage regardless of current. In this case the common mode voltage (noise and steady state) and ground loop voltage are similar to those that occur during the critical current measurement. There will still be some inductive voltage but the increasing and decreasing current portions should average to zero (for constant dI/dt). If the average is not zero, a ground loop or common mode voltage problem is evident. This test may be employed during an actual superconductor measurement. However, as in the dummy sample test, the voltmeter input leads must be connected to the same tap in order to simulate an ideal superconductor.
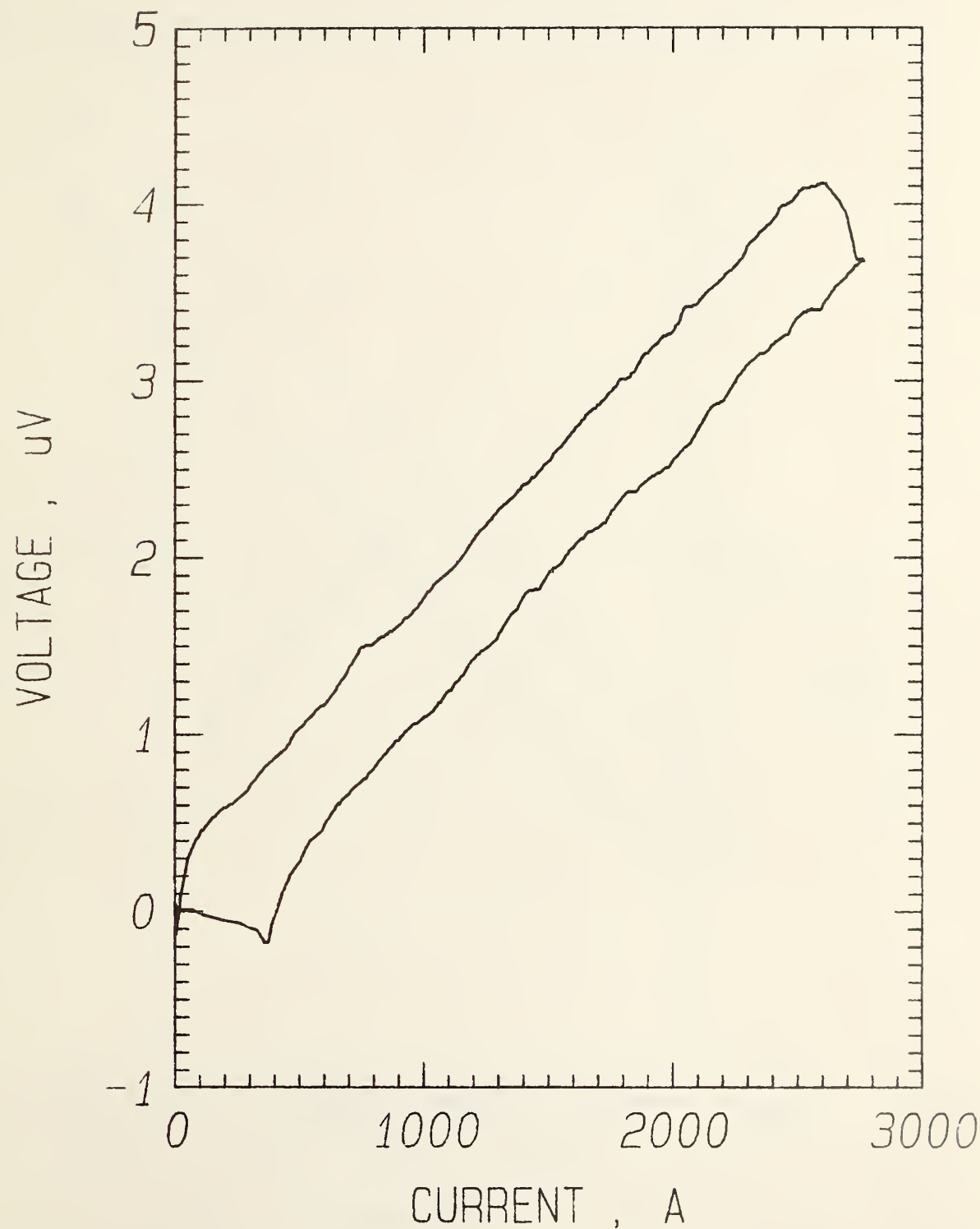
Figure 5. Finite resistance test, voltage versus current on a copper block using voltmeter A and a 3,000 A current supply.
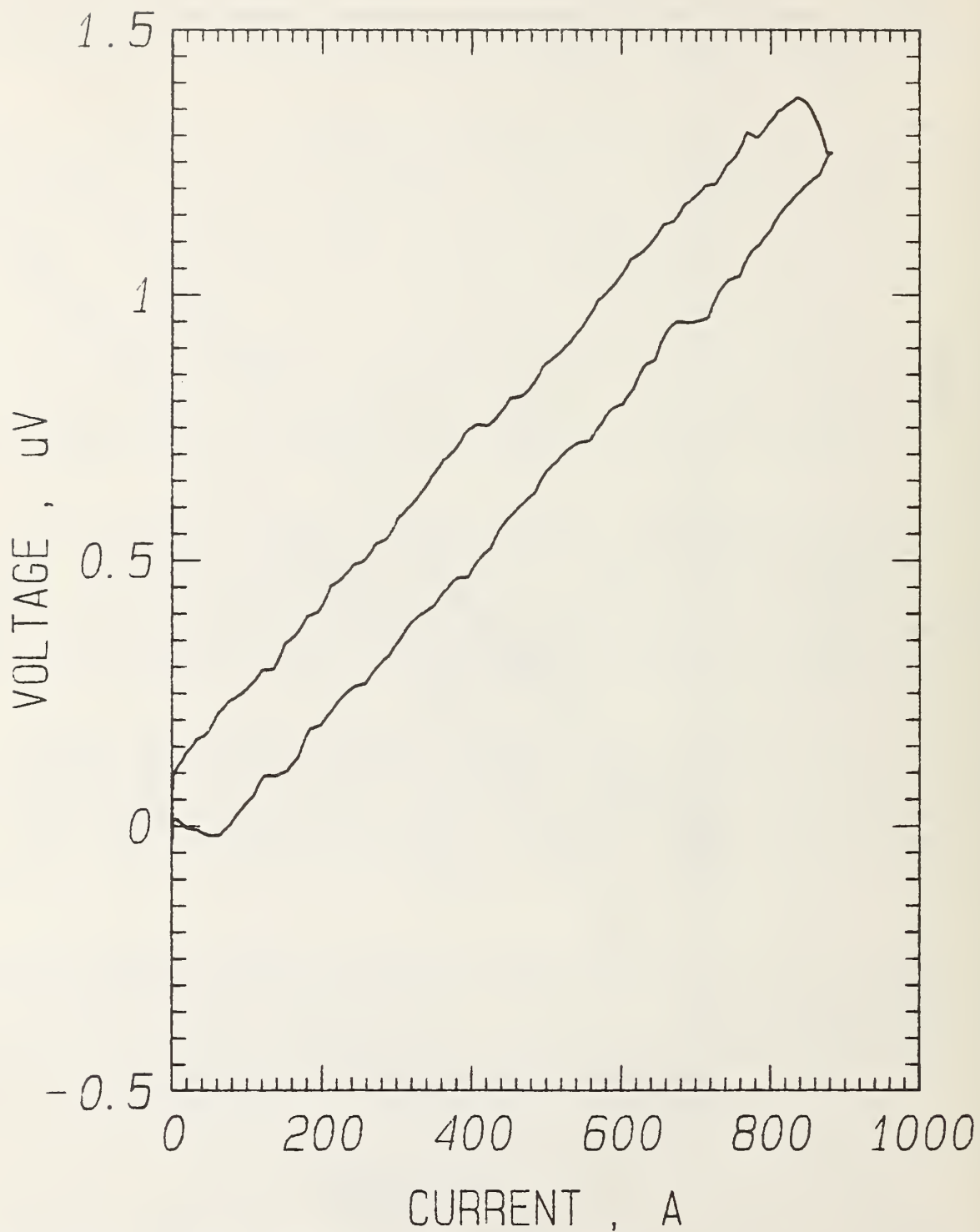
15

Figure 6. Finite resistance test, voltage versus current on a copper block using voltmeter A and a 900 A battery current supply.
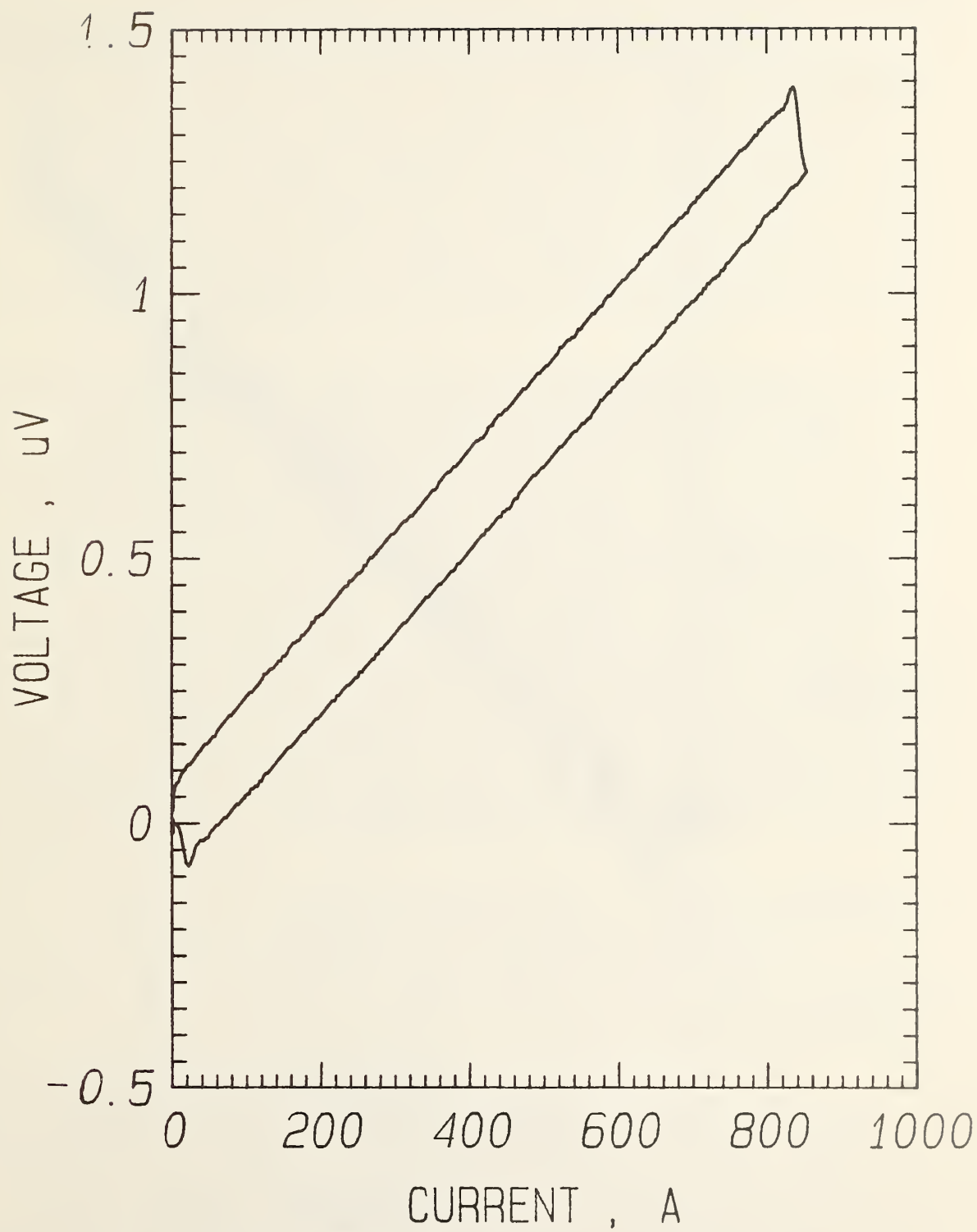
Figure 7. Finite resistance test, voltage versus current on a copper block
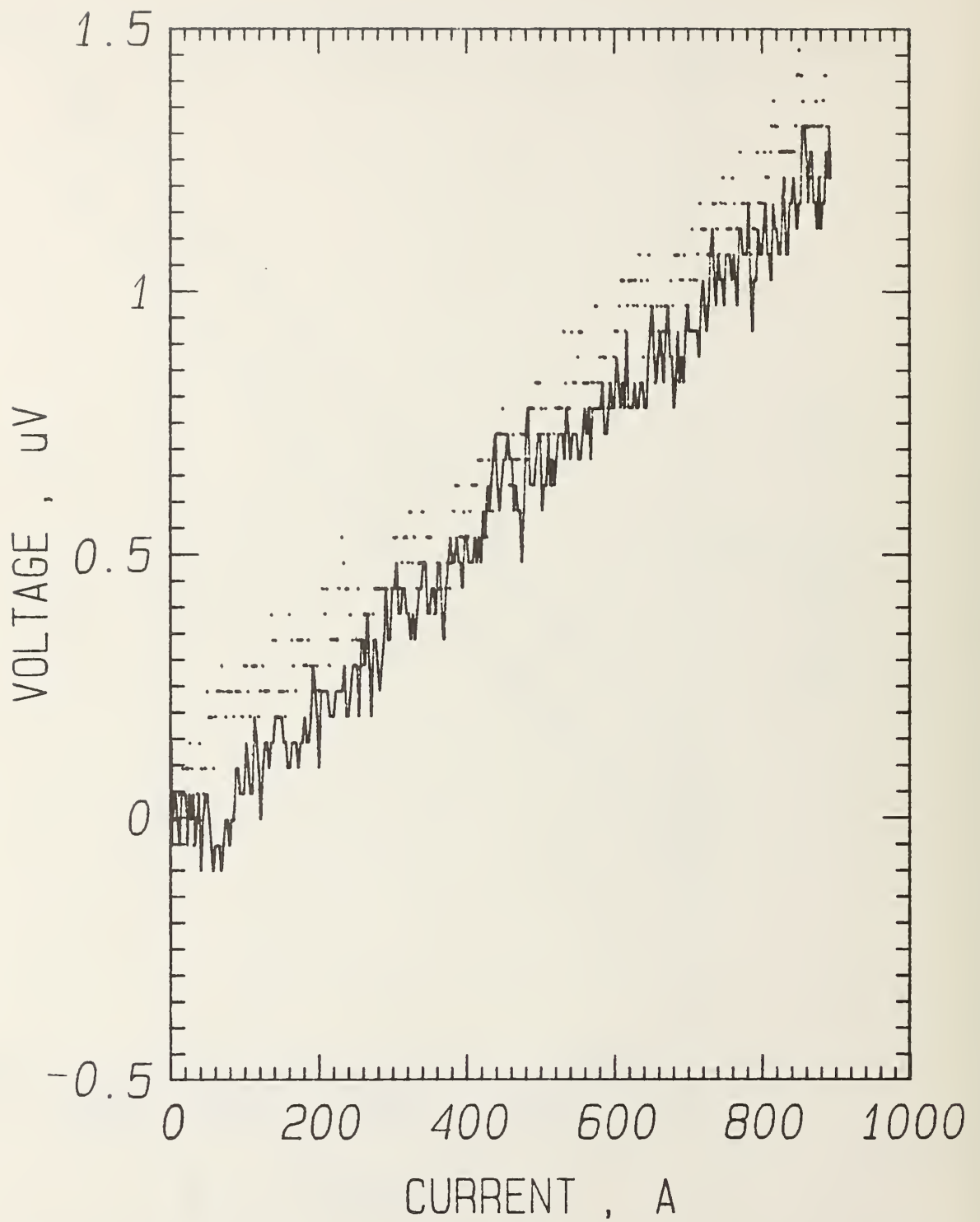using voltmeter B and a 900 A battery current supply.

Figure 8. Finite resistance test, voltage versus current on a copper block
using voltmeter C and a 900 A battery current supply with load grounded.

The ac and dc common mode voltages on the output of the two current supplies were measured from the load to ground with and without a ground connected to the load. The ground used in these tests was a good earth ground, not an ac power line ground. Without a ground on the load the voltage reference to ground is through leakage paths. For the 3000 A supply, the leakage path is mainly through the cooling water. In the battery supply the leakage path is not well defined but it does exist. The 3000 A current supply had a common mode voltage of about 6.4 V peak to peak and 1 V dc that was fairly independent of output current without a load ground. With a load ground, the common mode voltage increased with current from 2 mV peak to peak and 0 mV dc at low current to 5 mV peak to peak and 80 mV dc at 2500 A. The battery current supply had a common mode voltage on the order of 0.2 V peak to peak and 1 V dc that was fairly independent of output current without a load ground. With a load ground, the ac voltage was independent of current and was less than 1 mV peak to peak and the dc voltage increased with current from 0 mV dc at low current to 19 mV at 800 A.

Examples of this test for ground loop and common mode voltage problems are shown on figures 9-20 for three different voltmeters and two current supplies. All of these figures show meter voltage versus current for increasing (solid line) and decreasing (dotted line) current. The 3000 A current supply would jump up to about 500 A at turn on which results in a spike or lag in the voltage for this part of the curve. Voltmeter A, figures 9, 10, 11, and 12, was the only meter that passed the zero resistance test on both supplies regardless of load ground, however the noise level is fairly high (about 100 nV peak to peak). Voltmeter B, figures 13, 14, 15, and 16, did not pass this test on the 3000 A supply, although it was improved by the load ground in which case the false voltage was on the order of 100 nV. Without a load ground, the false voltage was on the order of 1 μV. Voltmeter B has the lowest noise level, 10 nV peak to peak, on the battery supply without a load ground. Voltmeter C, figures 17, 18, 19, and 20, had the most trouble with common mode voltage, giving about 230 μV of false voltage on the 3000 A supply without a load ground and 10 μV with a load ground. Voltmeter C had a small problem, 100 nV, with the battery supply without a load ground and was good with a load ground. In all cases the noise level was lower on the battery supply as expected.

The tests described above only provide a means of determining whether or not a measurement system is producing false voltages. Both common mode voltages (ac or dc) and ground loops may result in false voltages. Generalizations about the source of these problems cannot be made because they are system dependent. However, the value of these tests is not diminished by this fact. In our case adding a load ground reduced the common mode voltages and thus reduced the size of the effect.

Opto-isolators or optical couplers provide a good means of reducing ground loops in critical current measurement systems. Many power supplies, ramp generators, and voltmeters have a capacitor from the circuit common to ground. Some instruments have the circuit common connected directly to ground. Also in some types of testing, such as electromechanical, grounding the sample cannot be avoided. Optical coupling is now available in differential preamplifiers and in the amplified analog outputs of some digital voltmeters (see user notes on digital voltmeter section). They can also be incorporated into quench detectors (see appendix B). Optical coupling can
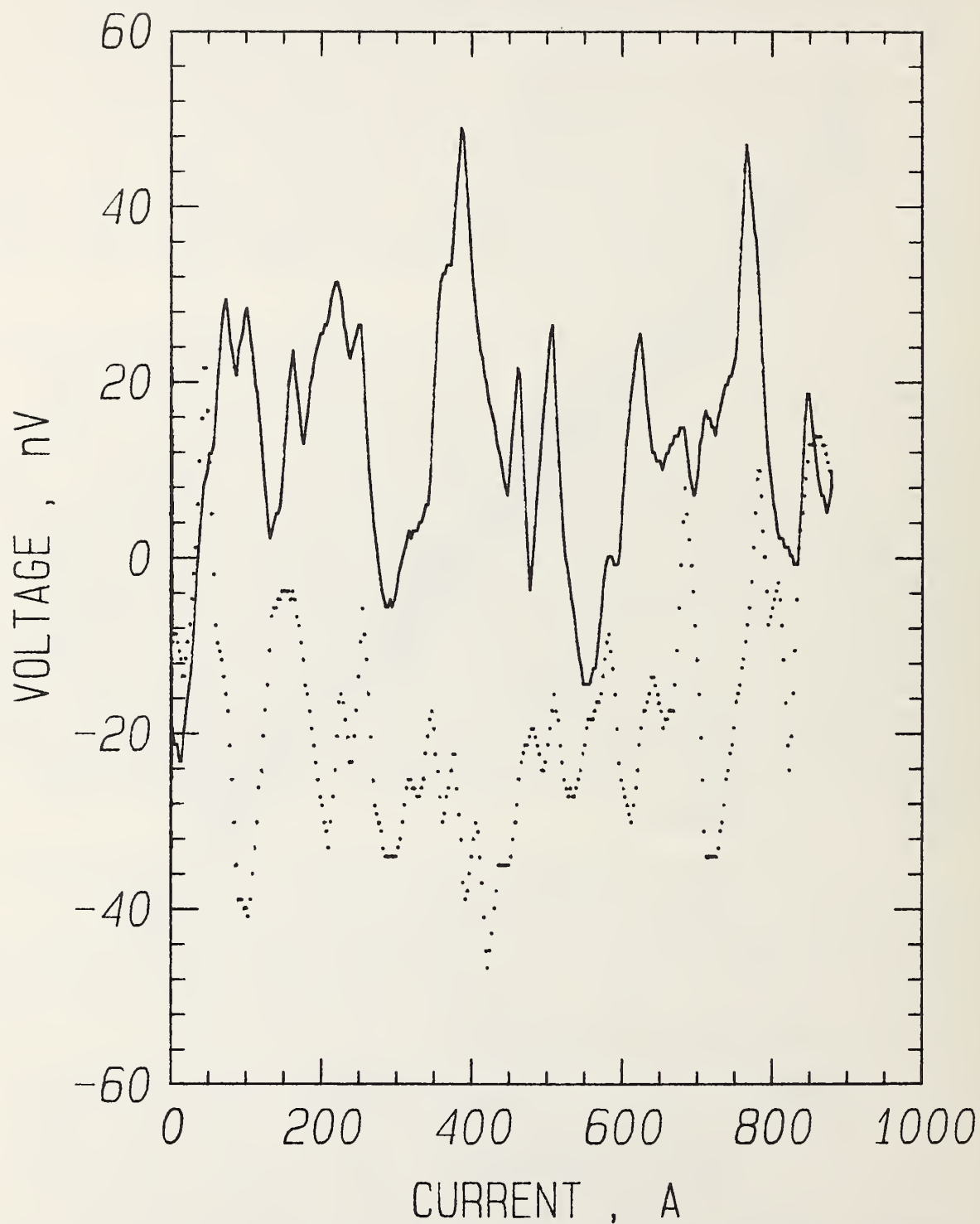
Figure 9. Zero resistance test, meter voltage versus current on a copper block using voltmeter A and a 900 A battery current supply.
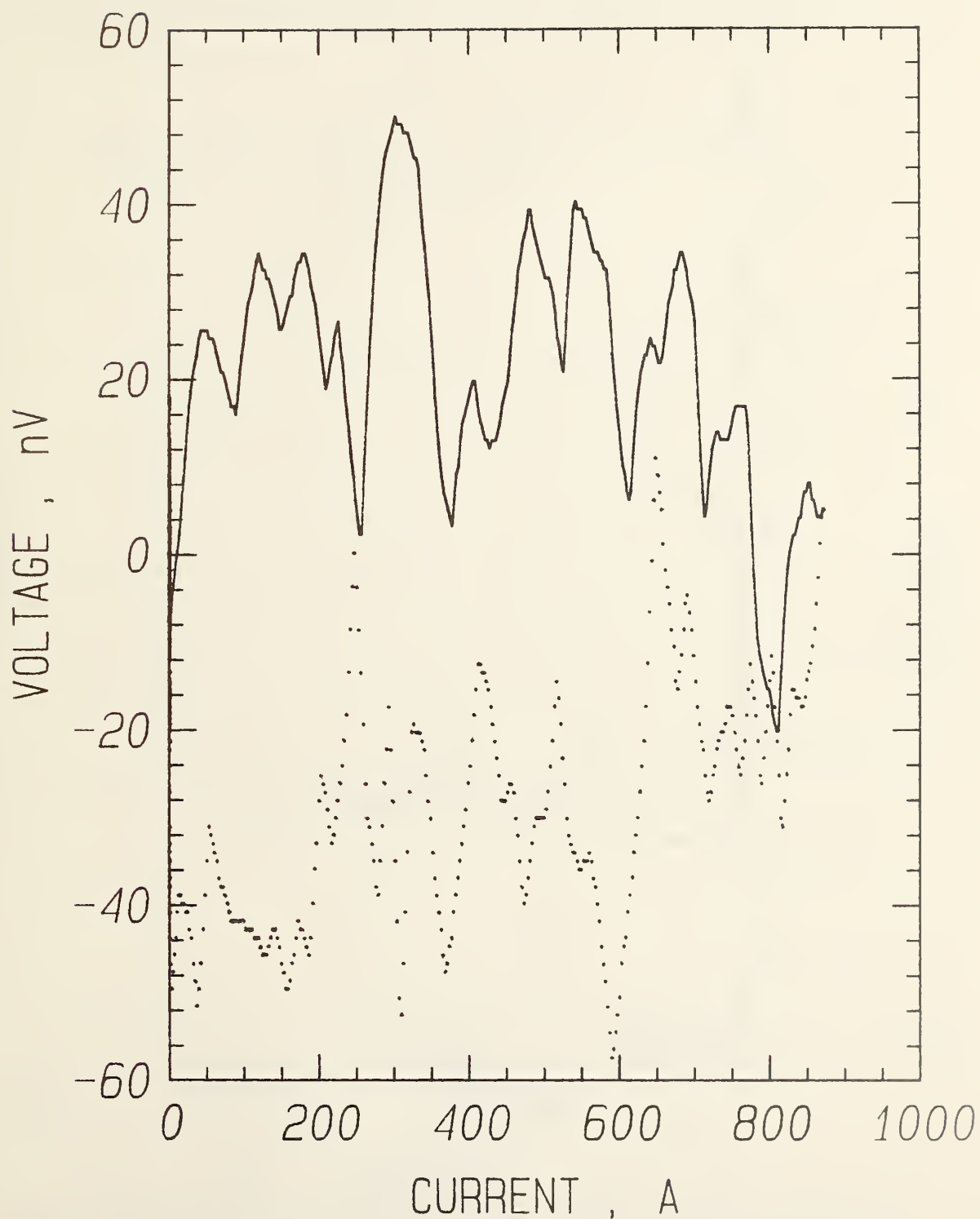
Figure 10. Zero resistance test, meter voltage versus current on a copper
block using voltmeter A and a 900 A battery current supply with load grounded.

Figure 11. Zero resistance test, meter voltage versus current on a copper block using voltmeter A and a 3,000 A current supply.

Figure 12. Zero resistance test, meter voltage versus current on a copper block using voltmeter A and a 3,000 A current supply with load grounded.

Figure 13. Zero resistance test, meter voltage versus current on a copper block using voltmeter B and a 900 A battery current supply.

Figure 14. Zero resistance test, meter voltage versus current on a copper block using voltmeter B and a 900 A battery current supply with load grounded.
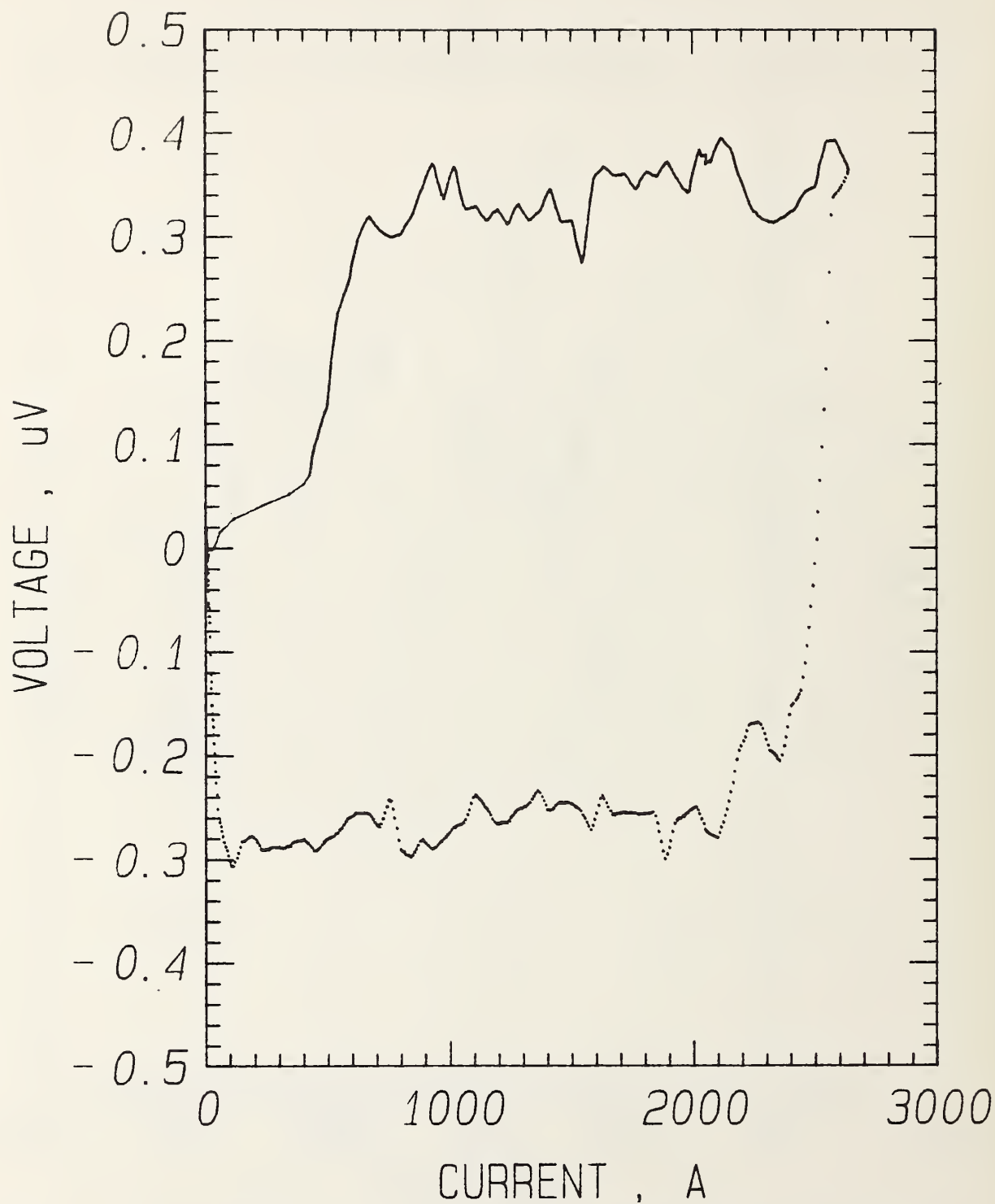
Figure 15. Zero resistance test, meter voltage versus current on a copper block using voltmeter B and a 3,000 A current supply.
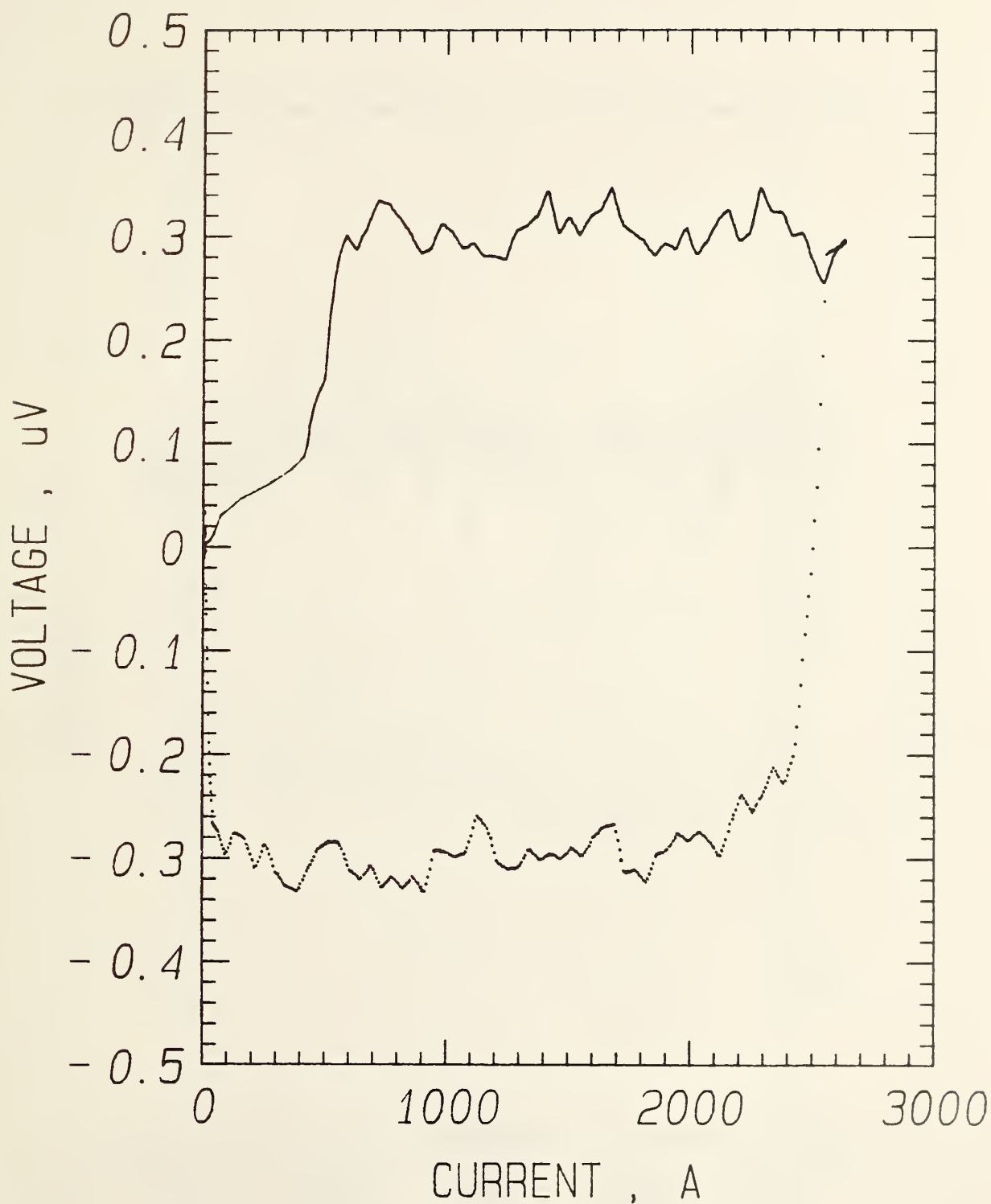
Figure 16. Zero resistance test, meter voltage versus current on a copper block using voltmeter B and a 3,000 A current supply with load grounded.
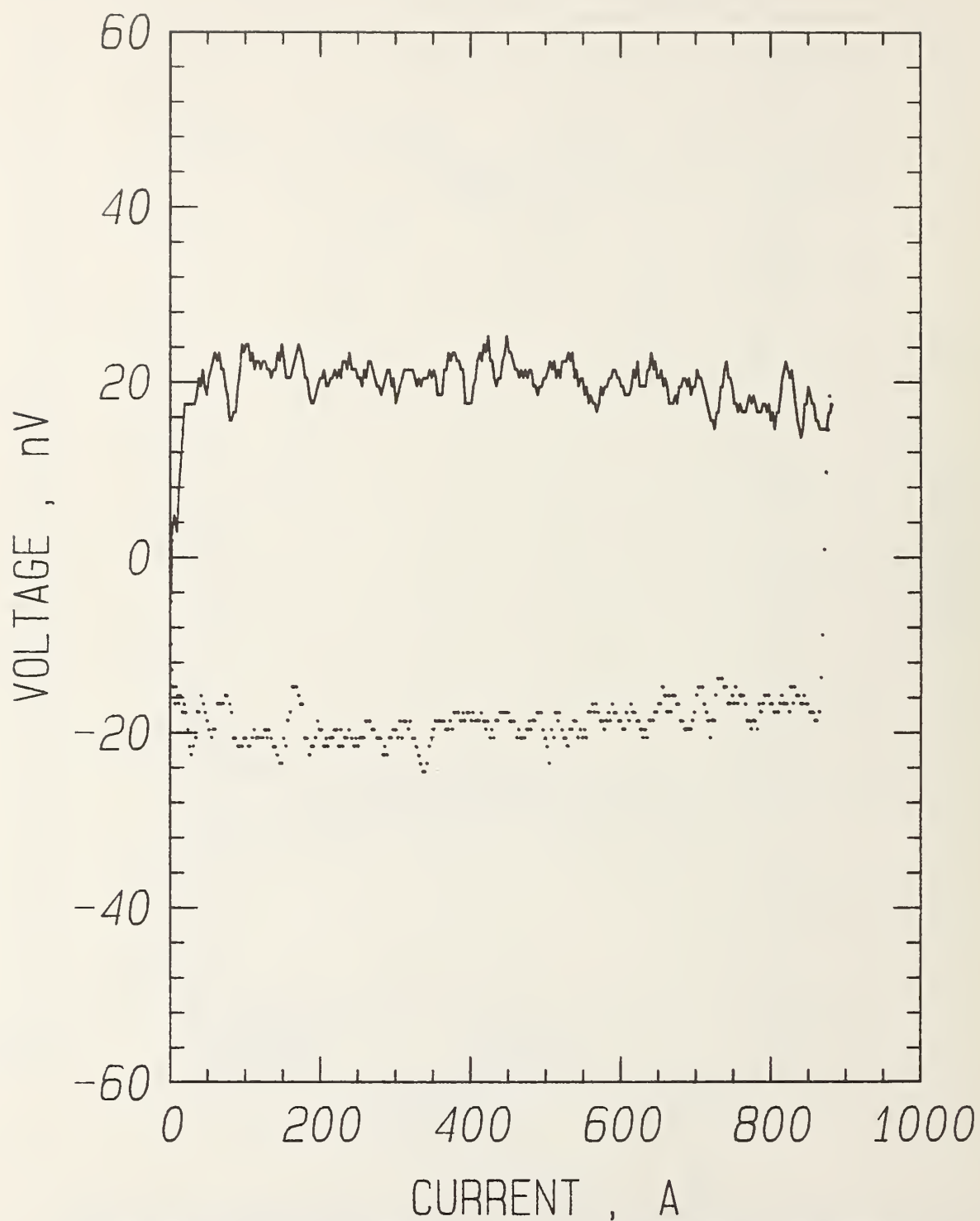
Figure 17. Zero resistance test, meter voltage versus current on a copper block using voltmeter C and a 900 A battery current supply.
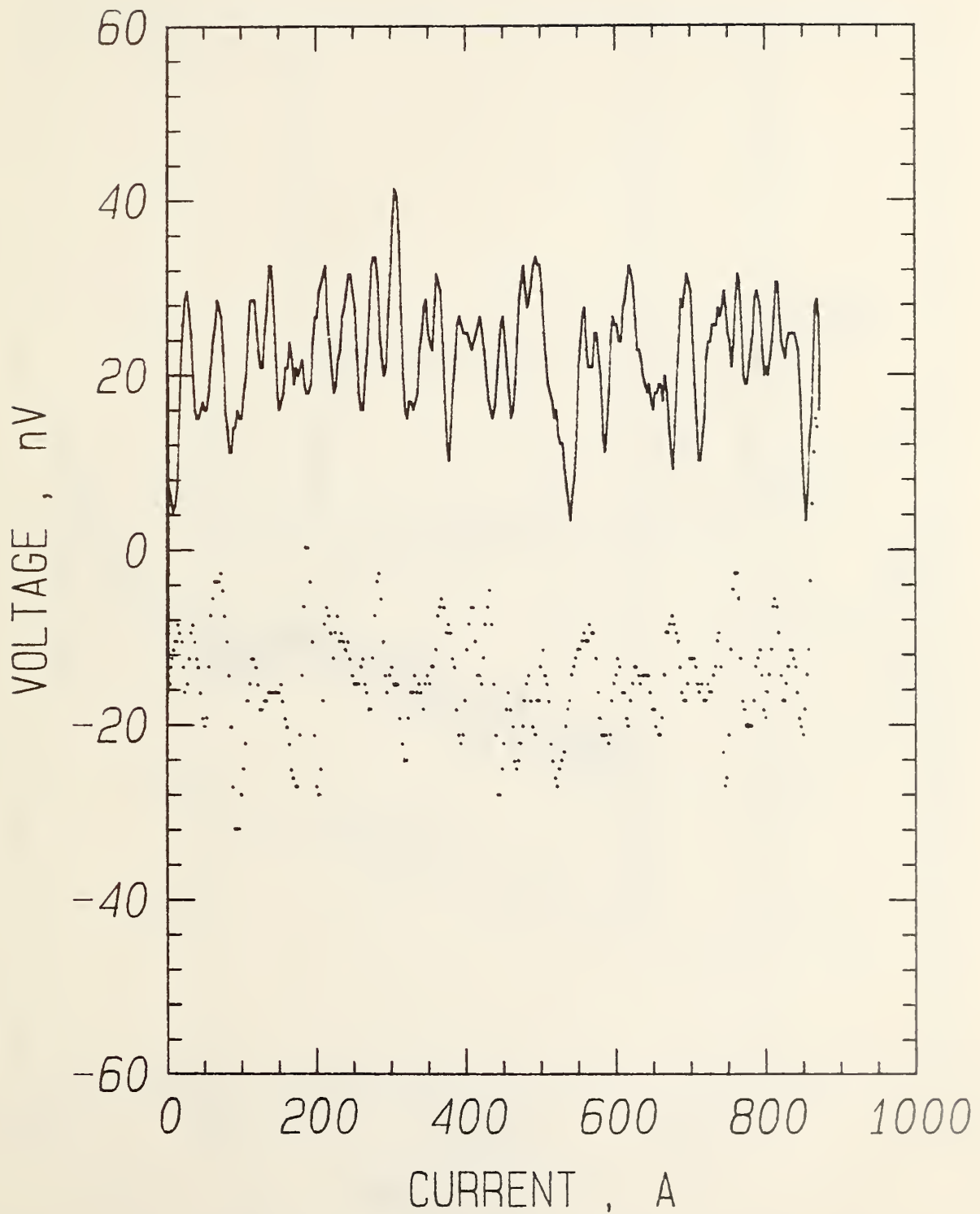
Figure 18. Zero resistance test, meter voltage versus current on a copper block using voltmeter C and a 900 A battery current supply with load grounded.
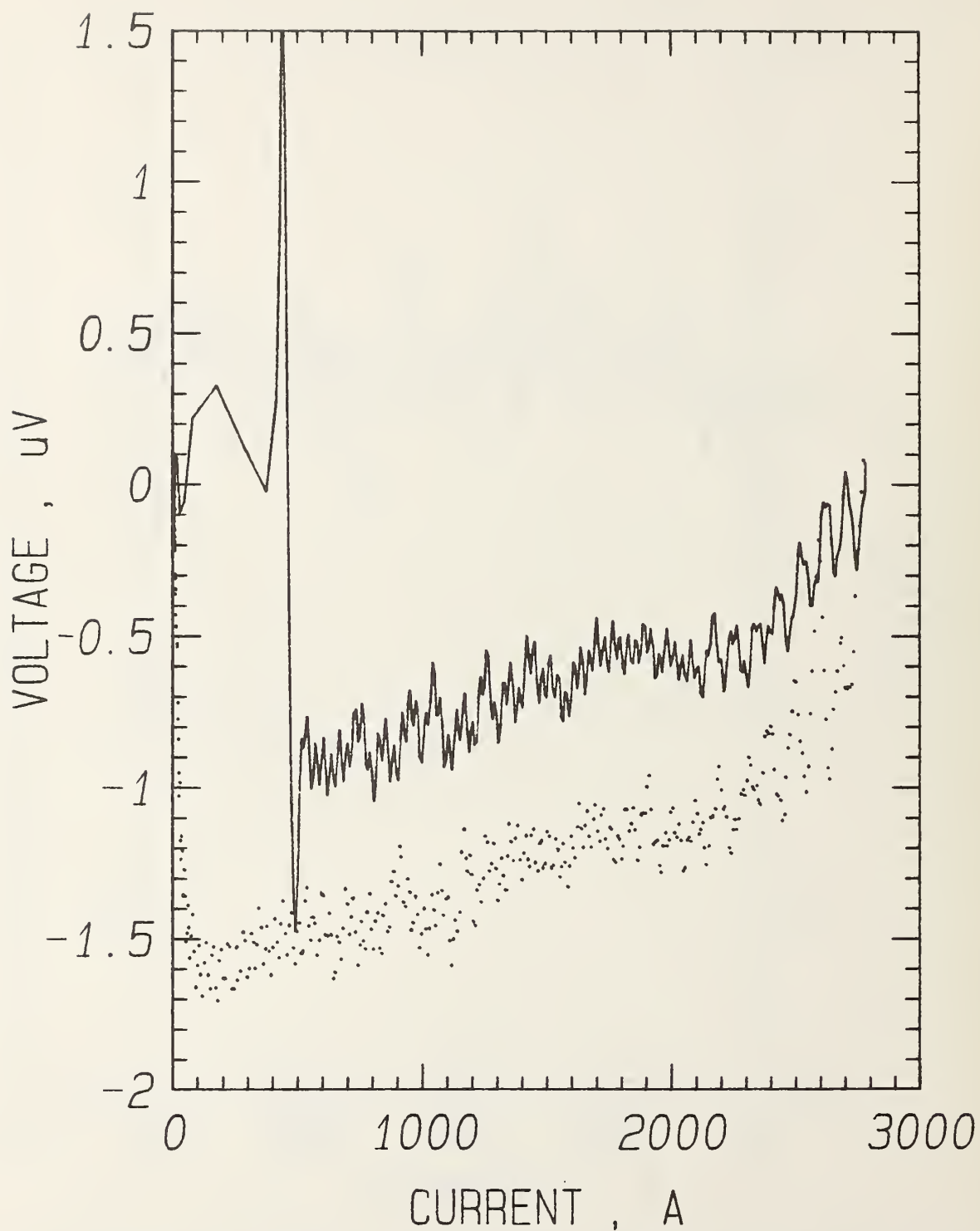
Figure 19. Zero resistance test, meter voltage versus current on a copper block using voltmeter C and a 3,000 A current supply.
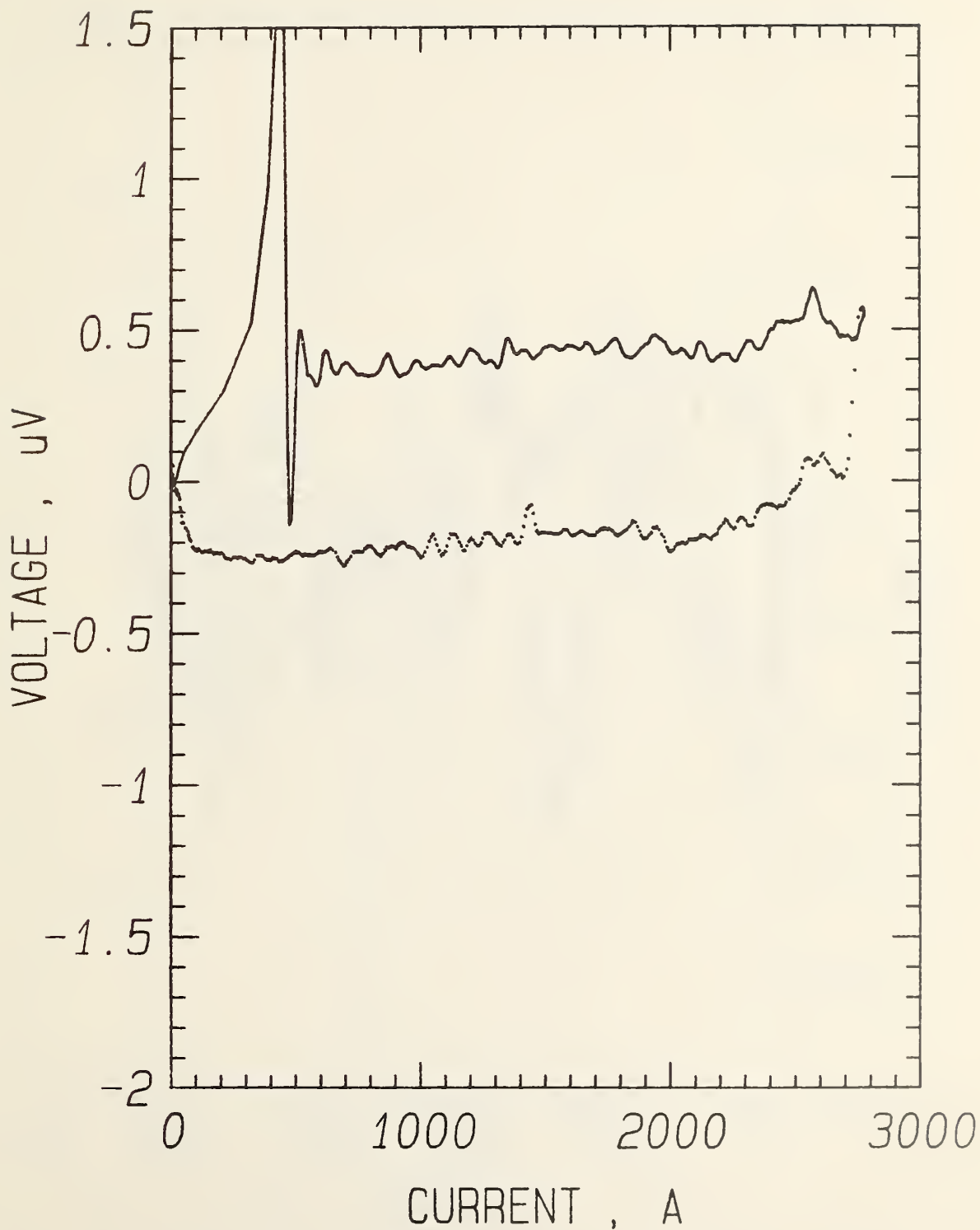
Figure 20. Zero resistance test, meter voltage versus current on a copper block using voltmeter C and a 3,000 A current supply with load grounded.
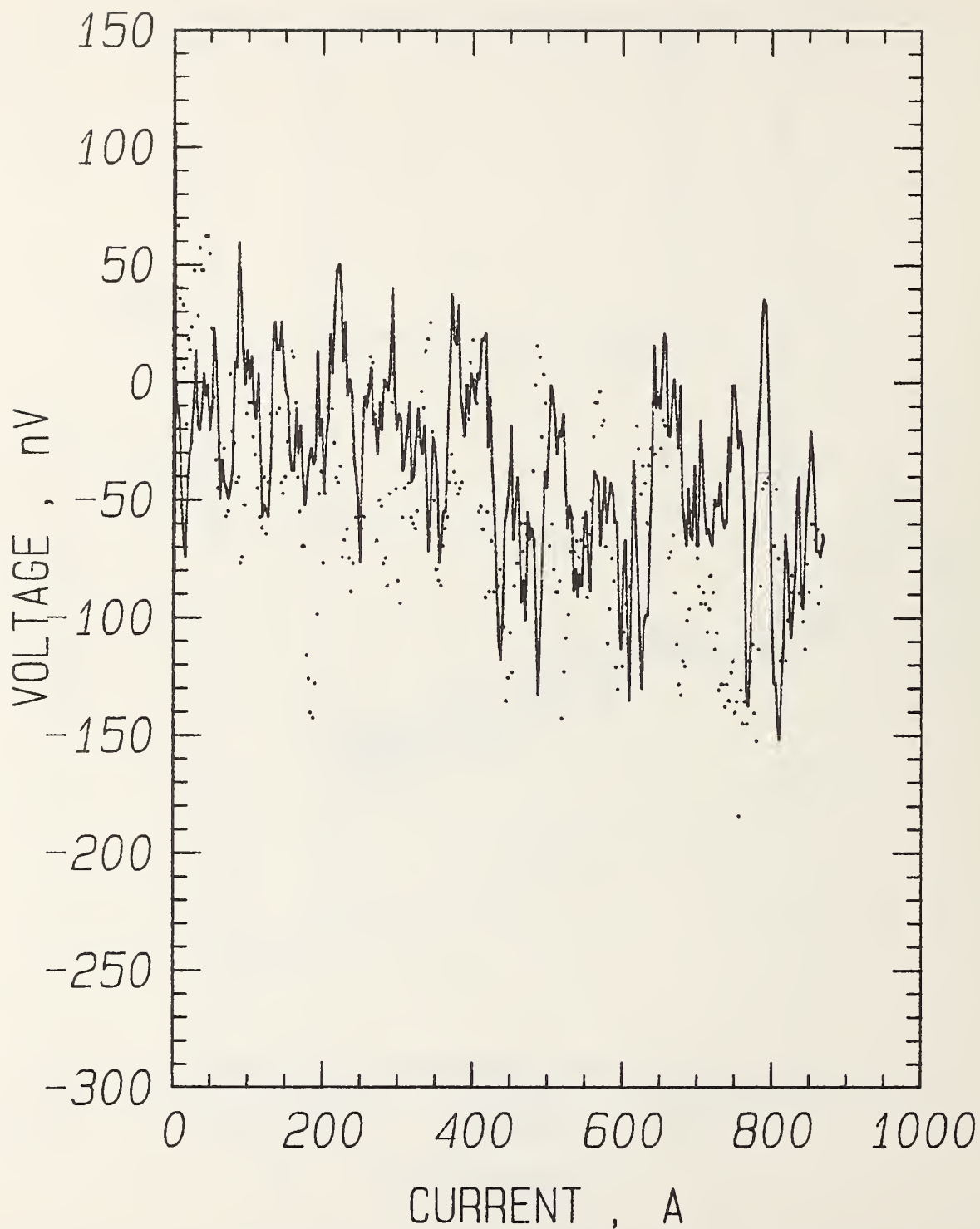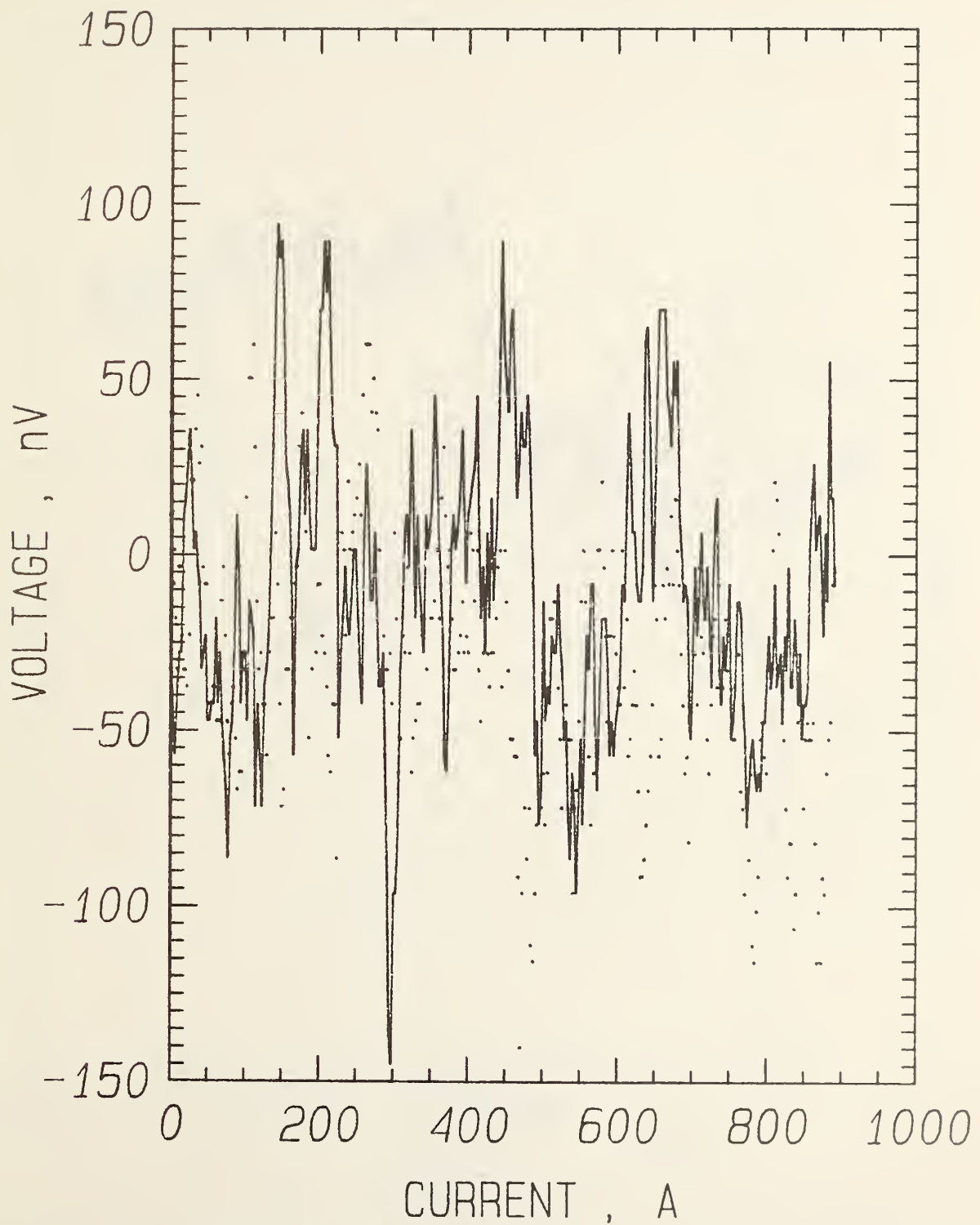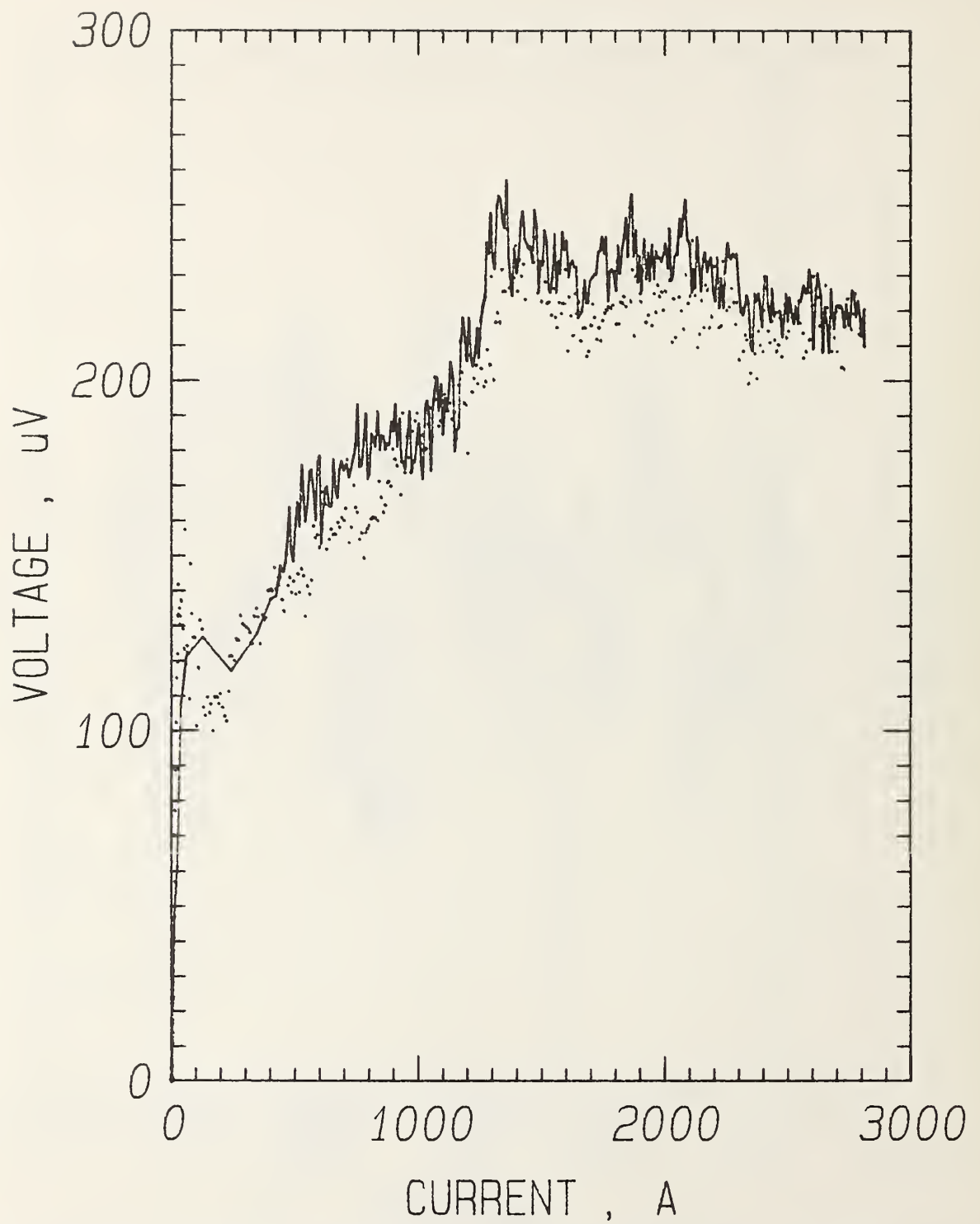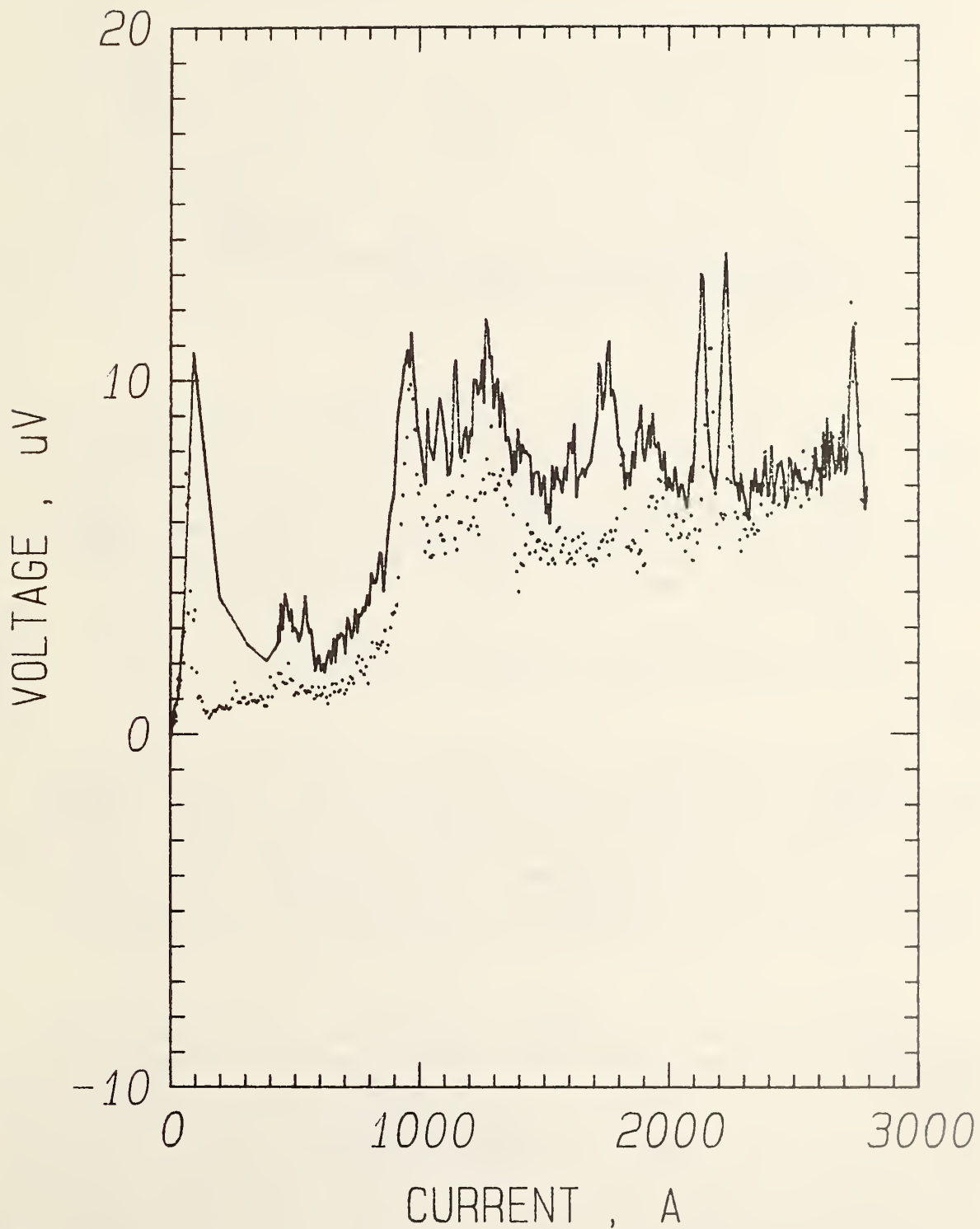
also be used between the ramp generator and a sample current supply (see section on battery powered current supply).

STABILITY

There are many theoretical stability criteria which fall into three categories: flux-jump stability, full cryostability, and limited cryostability. Flux-jump stability is based on the thermal diffusivity of the superconductor being greater than its magnetic diffusivity, so that a magnetic flux jump will not cause a thermal runaway event. The cryostability criteria are based on the power balance equation which compares the disturbance heat generation and joule heating to the cooperative effects of heat transfer to the cryogen, heat conduction, and heat storage. Each criterion corresponds to a solution to this equation with different simplifying assumptions. A magnet that has full cryostability will recover from a disturbance of any size, such as an infinite normal zone. A magnet that has limited cryostability will recover from disturbances of only a limited size.

The goals of this area of the research program are consensual definitions of terms and standard test methods. We have started to acquire the data base needed to create consensual standard test methods for the determination of stability parameters that are intrinsic to the wire and, thus, are figures of merit for the wire regardless of the details of the application. These variables could include resistivity, thermal conductivity, heat capacity, orientation-dependent surface heat transfer, and stability temperature margin. The stability temperature margin is calculated using $J_c(H,T)$.

The topics covered here are resistivity, copper-to-superconductor volume ratio, and critical current as a function of temperature.

Resistivity

We have the capability of routine resistivity ratio measurements of superconductors. The data acquisition and plotting is computer assisted. The measurement can be performed in a liquid helium shipping Dewar. The main complication of this measurement is determining the low temperature sample resistance just above the superconductive transition temperature in an easy and routine way. For the low temperature data, the resistance of a carbon resistor was used as an indicator of temperature. The sample and carbon resistances were measured at various positions in the shipping Dewar.

A typical set of data is given in figure 21. The resistance of the carbon sensor increases with decreasing temperature, so the temperature is decreasing to the right on the x-axis. There is a variation in the carbon resistance at which the superconductive transition occurs, because the sample and carbon sensor are not perfectly thermally coupled and the system is not in thermal equilibrium. However, this does not prevent a precise determination of the normal state resistance just above the transition. A more sensitive plot of these data in the plateau region allows for a resistance determination to within ±0.1 percent.
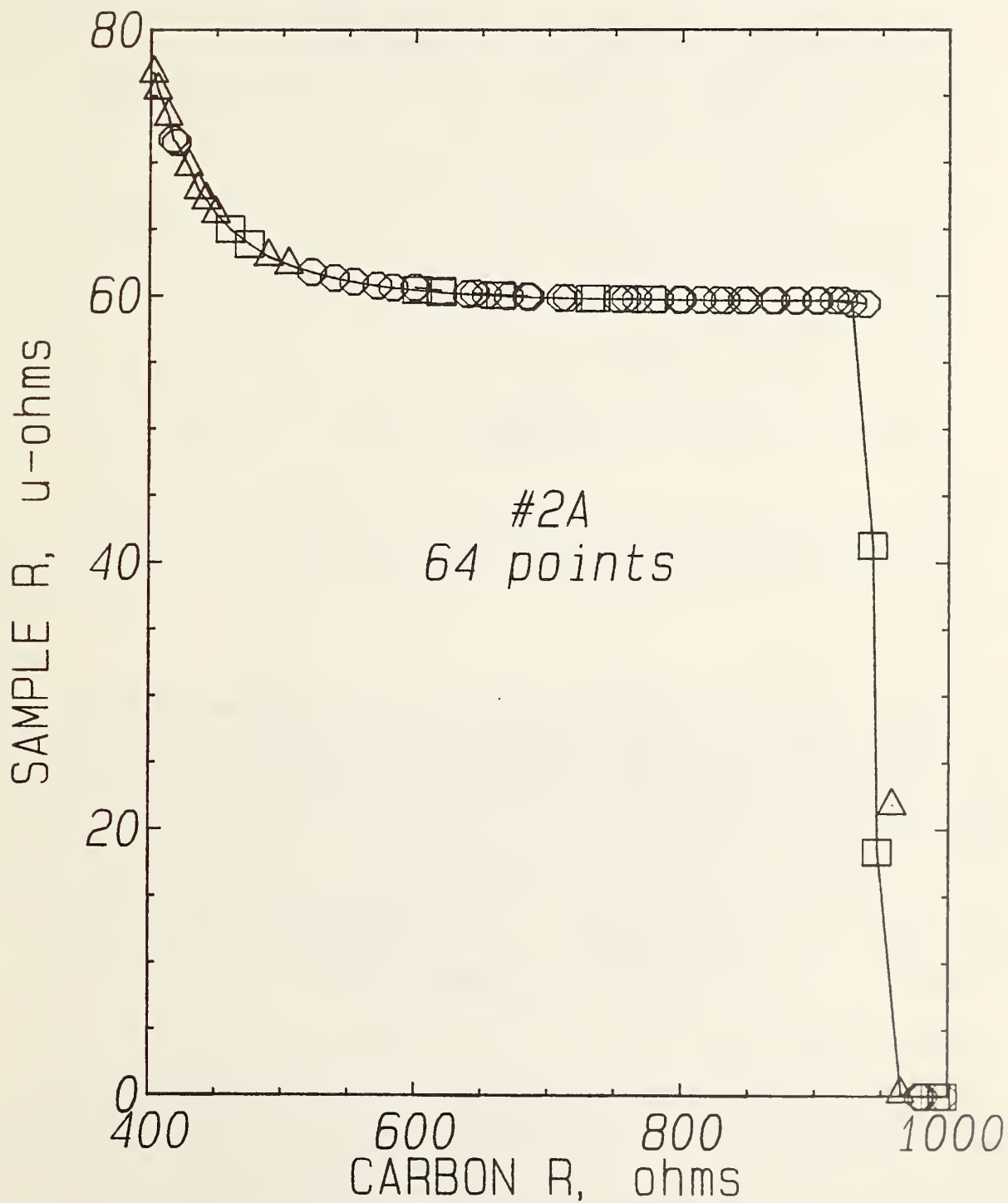
Figure 21. Sample resistance versus resistance of temperature sensing carbon
resistor (resistance of carbon resistor increases with decreasing
temperature).

A useful equation was developed which relates the copper residual resistance ratio (RRR) and the RRR of the composite superconductor. Start with the following definitions:

H is the composite resistance at room temperature,
C is the composite resistance at low temperature,
ρ_c is the room temperature resistivity of the copper,
ρ_s is the room temperature resistivity of the non-copper material,
A_c is the area of the copper,
A_s is the area of the non-copper material,
R is the resistance of the copper at room temperature,
x R is the resistance of the non-copper material at room temperature,
w is the RRR of the composite (H/C),
y is the RRR of the copper,
z is the RRR of the non-copper material,

where $x = (\rho_s A_c)/(\rho_c A_s)$.

Then

$$H = xR/(x+1) \quad \text{and} \quad C = xR/(xy+z);$$

therefore

$$w = (xy+z)/(x+1)$$

and thus

$$y = w + (w-z)/x.$$

The last equations involve dimensionless variables using these definitions. In the limit that x goes to infinity, y approaches w. In the limit that z goes to w, y also approaches w. For most composite superconductors; y, copper RRR, will be greater than w, composite RRR.

Copper-to-Superconductor Volume Ratio

A careful study of assumptions and technique was done on the copper-to-superconductor volume ratio measurements as part of another program in our group at NBS. This other research is on transient losses in superconductors for the Air Force Office of Scientific Research [10].

Stability Apparatus

As part of another program an apparatus to study stability has been constructed and preliminary measurements performed. This other research is on copper stabilizers in superconductor for the International Copper Research Association by F. R. Fickett. In collaboration, preliminary measurements of the critical current as a function of temperature are being made. Calibrations of the thermometers in magnetic field have been made. A publication is in process.

STANDARD REFERENCE MATERIAL (SRM)

The small conductor (NbTi) critical-current SRM (No. 1457), and further advertisement of the critical current standard test method (ASTM B714-82) will help all critical current measurements. As the technology matures, other critical current and stability SRM's will be useful. Possible critical current SRM's that may be useful are: large conductor monolithic NbTi, large conductor NbTi cable, and small or large Nb_3Sn conductors. Magnet designs may need some settling time and more understanding before a stability SRM can be developed.

The cost of producing an SRM involves more than the purchase of material and its characterization. There are costs to refine the characterization technique to achieve accuracy and precision levels beyond those of an ASTM standard in order to reduce the overall uncertainty of the SRM. There are also costs associated with preliminary screening of candidate materials in order to pick the one best suited for this application. Limited funding is sometimes available from the Office of Standard Reference Materials (OSRM) to produce SRM's, but the total cost of development must be passed along to the consumer. The research to develop an SRM must be subsidized with money from NBS and other interested users such as DoE.

Our choices and direction for the SRM development program will be based on recommendations and feedback from ASTM committee members (B01.08) and the research community. Some of the topics to follow address these issues and our present ideas.

Nb_3Sn

A Nb_3Sn SRM may now prove quite useful, although this material presents additional problems. The problems of current transfer voltage, reaction conditions, and strain sensitivity would make this very difficult. An argument can be made that, for these reasons, a Nb_3Sn SRM should not be developed yet. The counter-argument is that it should be done for these very reasons, assuming it can be done. The difference is in the philosophy of its usage. Should an SRM check out the measurement system or technique? If a laboratory makes measurements on Nb_3Sn then it is dependent on its technique, including all of the extra measurement problems that Nb_3Sn has.

If a Nb_3Sn SRM can be produced, it would provide calibration to higher magnetic fields. With a 12 T magnet on order, we would plan to certify to that field. The capacity of the conductor would most likely be at or below 600 A at the lowest certified magnetic field, which at this point is thought to be in the range of 4 to 6 T. This would provide some overlap in field with the NbTi SRM. As was done with the NbTi SRM, additional non-certified measurements could be made at higher magnetic fields and as a function of strain. Since these measurements are not done on site, the control, time, and statistics are not adequate for certification.

The state of the art in Nb_3Sn conductors is not perceived as being as mature as NbTi was when it was developed, especially in terms of critical current homogeneity. Other concomitant variables are current transfer length, reaction schedule, irreversible strain, and strain sensitivity.

Large Conductor NbTi

The potential benefits of another NbTi SRM would either be much higher current or higher homogeneity. At this point the possible quantum improvement with higher homogeneity is not significant. However, there is adequate margin for increasing the current level with our present capabilities, 3000 A. The small SRM's critical current was 300 A at 2 T and 75 A at 8 T. We could increase this by a factor of ten (or 15 if we start at 4 T). A higher current SRM would allow for calibration of high current test facilities.

The choice between cable and monolithic conductor depends on bias introduced by the latest magnet design and some questions similar to those raised on the Nb_3Sn, ease versus reality. Most of the big magnet designs now use cable conductors. Cable conductors are more difficult to measure with the concerns about gauge length, local variations in critical current, and current transfer among strands. As in Nb_3Sn, that may be the reason for developing a cable SRM, if it can be done.

Two other fundamental questions are cost and number be used. The number of potential users decreases as the current level increases. Also the material and testing cost would be much higher for a larger conductor.

Self-Field

This topic is an open question: should critical current measurements be corrected for self-field? This topic is of concern for an SRM but it is also important for a large conductor test method. Self-field is the magnetic field produced by the transport current of a conductor. For the first SRM, we did not make a self-field correction because the same field is present for all measurements made with transport current. We did attempt to make a smaller correction for the magnetic field produced by the geometry of the test sample (inductive coil). This was done to correct to the more ideal case of a long straight wire.

There are times when a self-field correction is important such as in comparing the current density of different size wires or single strand to cable measurements [11]. The effect will be more significant for the larger conductors and is a bigger source of error whether the correction is done or not. The answer is not obvious.

European Economic Community Wire

We made some measurements of critical current on a wire provided by the European Economic Community. This was a NbTi wire that was used in their round robin testing and put forth as a reference material. We were interested in comparing round robin measurements and determining whether this wire had short range variation similar to SRM 1457.

This reference material was selected based on its parameters and availability [12]. This is a simple conductor of which many tons had been produced. The wire has 24 filaments (66 μm diameter) arranged equidistant on the same radius to reduce internal current transfer problems. Other conductor parameters are: copper-to-superconductor ratio of 7.44, insulated wire diameter 1 mm, uninsulated wire diameter 0.94 mm, and filament twist pitch of

45 mm. This conductor was believed to have high homogeneity, little variation in superconductive properties. A round wire avoids differences in critical current with rotation of the magnetic field vector around the wire axis. A high copper-to-superconductor ratio will increase cryogenic stability.

Seven European laboratories made measurements on specimens of this wire [13]. Measurements were made at magnetic fields from 0 to 10 T, but not all of the participants reported critical currents at all of the integer values of magnetic field. Vacuumschmelze made additional measurements on specimens adjacent to the specimen of each participant. Rutherford Appleton Laboratory made three sets of measurements making a comparison among specimens that were held on the test fixture with; oil (insulation left on the wire), solder, and a specimen that was removed and soldered again.

Table 1 has a summary of the critical currents, percentage range of reading, and number of readings (including the multiple measurements). The percentage range of critical currents seems to increase with magnetic field from 2 to 6 T. The smaller than expected range at 8 T is probably due to the lower number of readings taken there. These data in the range of 4 to 8 T were fit to a linear relationship of current with field. The current and magnetic field intercepts were used to compare the respective calibrations. This assumes linear calibration differences. If all of the differences among these data were due to calibration differences only, the differences would have to be ±3 percent in current and ±2 percent in magnetic field. Vacuumschmelze's measurements on 6 specimens indicated that the wire properties vary by about ±2 percent in current and ±1 percent in magnetic field. This type of analysis was not done on SRM 1457 but it would be similar.

Some of the conclusions of the European laboratories [13] were that the range of critical currents were due to variations in: the sample, the method of mounting and measurement, and the sample temperature. The attempt to normalize the measurements with the Vacuumschmelze adjacent specimen did not reduce the deviations, indicating that the sample variation was significant over the length of a meter. The results of the Rutherford Appleton Laboratory study indicated a possible progressive 1 percent reduction with soldering a specimen. Also the absolute pressure of the cryostat should be recorded.

The measurements at NBS on this wire were not included in the above mentioned study, but our results were consistent with theirs. The measurements at NBS were made on two sample holders in the same background magnet. The geometry of the two holders were an inductive coil and a short straight. Table 2 has a summary of these measurements with critical currents and percentage differences. The coil values are within 2 percent of the average European value. The difference between coil and short straight is probably due to a bending strain effect. The bending strain effect was expected to be large because the wire diameter is relatively large and most of the filaments are off the neutral axis.

Three pairs of voltage taps were placed on the coil sample to determine the short range variation in critical current. The tap separation of each pair was 2 cm. Adjacent pairs were separated by about 10 cm. The percentage range of critical current values increased monotonically with magnetic field

37

Table 1

Summary of critical current measurements by European Economic Community on their reference material.

Magnetic Field T	No. of Readings	Average Critical Current, A	Percentage Range
2	15	332.1	4.5%
4	17	225.7	6.2%
6	17	144.9	10.4%
8	6	68.5	5.3%

Table 2

Summary of critical current measurements by NBS on European Economic Community
reference material.

Magnetic field, T	I_c, A on coil holder	I_c, A on straight holder	Percentage of reference between coil and straight	Short range between variation on coil
2	332.5	342.6	2.9%	0.62%
4	227.2	234.1	2.9%	0.81%
6	147.4	152.3	3.2%	1.01%
8	67.6	71.1	4.9%	1.39%

from 0.6 percent at 2 T to 1.4 percent at 8 T. These short range variations are similar to those observed in the preliminary screening of standard reference materials at NBS.

Nb_3Sn Round Robin

We participated in the USA (DoE) and Japan round robin to measure the critical current of two select multifilamentary Nb_3Sn conductors. This was the first attempt at international standardization of the measurement of critical current for this important class of high magnetic field superconductors. The goal of this round robin was to determine the degree of agreement among measurements made in different laboratories and identify sources of any disagreement. Six U.S. laboratories and six Japanese laboratories made critical current measurements. Additional measurements of homogeneity and temperature dependence of critical current were performed and evaluated by NBS for each conductor. This information will be useful in deciding the course of the NBS superconducting wire Standard Reference Material program.

We need to make further evaluations before we can draw conclusions. A discussion of the results and summaries were presented to the community by some of the participants at the Fourth U.S.-Japan Workshop on Superconducting Materials for Fusion, Feb. 26-28, 1986 in Hedgesville, West Virgina. The range of measured values for the U.S. participants [14] was 14 percent at 8 T and 20 percent at 12 T.

SUMMARY

Progress has been made on recognizing, understanding, and in some cases reducing the effect of experimental difficulties that are substantial for large conductor critical current measurements. The basic characteristics of the current supply and voltmeter have a major role in the precision and accuracy of the measurement. A simple test method was outlined which can be used to test the system integrity. In conjunction with this progress, there have been two publications during this reporting period, Appendices A and B. Preliminary efforts have been made in stability and future Standard Reference Materials. The overall result of this work has been an increase in funda-mental understanding, technology base, and experimental capabilities.

ACKNOWLEDGMENTS

REFERENCES

[1] L. F. Goodrich, D. F. Vecchia, E. S. Pittman, J. W. Ekin, and A. F. Clark, "Critical Current Measurements on an NbTi Superconducting Wire Standard Reference Material," NBS Special Publication 260-91 (1984).

[2]   L. F. Goodrich, W. P. Dube, E. S. Pittman, J. W. Ekin, and A. F. Clark, "The Effect of Aspect Ratio on Critical Current in Multifilamentary Superconductors," Adv. Cryo. Eng.-Materials, Vol. 32, Plenum Press, New York (1986).

[3]   W. P. Dube and L. F. Goodrich, "Quench Detector Circuit for Superconductor Testing," Rev. Sci. Instrum., 57, 680-682 (1986).

[4]   J. W. Ekin, National Bureau of Standards, Boulder, Colorado, private communication.

[5]   This work was originally presented informally at the 4th Workshop on NbTi Superconductors (July 1985 Madison, Wisconsin). Discussions are acknowledged, especially with C. King, Intermagnetics General Corporation, Guilderland, New York.

[6]   J. W. Ekin, National Bureau of Standards, Boulder, Colorado, private communication.

[7]   A. C. Rose-Innes, Low Temperature Laboratory Techniques, English Universities Press Ltd., London, 1973.

[8]   M. M. Kreitman, "Simple Diaphragm Pressure Regulator for Cryogenic Bath Temperatures," Rev. Sci. Instrum., 35, 749-750 (1964).

[9]   J. E. Ostenson, Ames Laboratory, Ames, Iowa, private communication.

[10] R. B. Goldfarb, "Transient Losses in Superconductors," NBSIR 86-3053, National Bureau of Standards, Boulder, Colorado (June 1986).

[11] M. Garber and W. B. Sampson, "Critical Current Anisotropy in NbTi cables," IEEE Trans. on Magnetics, MAG 21, 336, 1985.

[12] European reference material provided by K-J. Best of Vacuumschmelze, Hanau, West Germany.

[13] C. R. Walters, Rutherford Appleton Laboratory, Oxfordshire, England, private communication.

[14] D. C. Larbalestier, University of Wisconsin, Madison, Wisconsin, private communication.

THE EFFECT OF ASPECT RATIO ON CRITICAL CURRENT IN MULTIFILAMENTARY

SUPERCONDUCTORS *

L. F. Goodrich, W. P. Dube, E. S. Pittman, and A. F. Clark

National Bureau of Standards
Boulder, Colorado

ABSTRACT

Experimental data and discussion are presented on the critical current of straight superconductors as a function of the orientation of a perpendicular applied magnetic field. Commercial, multifilamentary NbTi and Nb_3Sn samples were measured in a radial access magnet that allowed an arbitrary angle setting. The change in critical current was measured at different magnetic fields to scale the effect for use in a standard test method. For a NbTi sample, the critical current with the magnetic field parallel to the wider face of the conductor is higher than that with the perpendicular orientation. The effect can be as high as 40% for a NbTi sample with an aspect ratio of six. The effect in Nb_3Sn is opposite that in NbTi. A discussion of the most likely cause of the effect, which accounts for the difference between NbTi and Nb_3Sn, is given.

INTRODUCTION

The aspect ratio effect is defined as the variation of critical current, I_c, with sample-field orientation in a constant applied magnetic field perpendicular to the wire axis. The aspect ratio of a conductor or filament is defined as the ratio of the cross sectional dimensions (wide/narrow). The emphasis of this study was measurement of how the critical current varied with the angle of constant applied magnetic field. The most likely cause of the aspect ratio effect is the asymmetric deformation of the filaments and, thus, the orientation of the flux-pinning sites.

The aspect ratio effect on critical current is important for most applications where a monolithic rectangular conductor is used. It may also be of importance for understanding the critical current of cable conductors that have been deformed during compaction. The difference in I_c can be 20% for a NbTi conductor with an aspect ratio of two (40% for a ratio of six). The present American Society for Testing and Materials (ASTM) critical current standard test method[1] suggests a measurement orientation with the magnetic field parallel to the wider face of a rectangular sample unless otherwise specified, but this orientation is difficult to obtain in the

hairpin geometry. Also, in some applications, such as the end turns of a dipole magnet, might require the measurement in the other (or both) orientations.

EXPERIMENTAL

The critical current measurements reported here were made using a straight sample geometry and a radial access magnet. Samples are identified in Table 1. The critical current was defined as the current at which the electric field strength was 0.2 μV/cm. The sample was centered in a holder, and four conductors (symmetrically located on a 2-cm diameter circle) were used for the return current path. This arrangement reduced the effect of the magnetic field from the return current path and reduced the net torque on the sample cryostat. The sample was held in, and electrically isolated from, a machined brass rod holder with epoxy. The rest of the structure was fiberglass epoxy.

Two experimental problems were identified and their effects on precision and accuracy reduced. The first was voltage noise, as large as several μV, introduced by slight motion of the sample during acquisition of the voltage-current (V-I) curve. The net force on the sample cryostat is not zero if the current return path does not traverse exactly the same magnetic field profile as the sample path. Additionally, stray Lorentz forces and mechanical vibrations can cause relative motion of the magnet and sample. The noise problem was reduced to the 0.1 μV level with the addition of a band brake device that was mounted on the top of the magnet. This brake could be tightened around the sample cryostat with a room temperature screw actuator, thus restricting the relative motion of the magnet and sample.

The second problem was persistent currents in the four parallel return wires, because the wires were soldered together at each end and the magnetic flux was changed each time the angle was changed.[2] These persistent currents would cause a time dependent, partial shielding of the sample from the applied magnetic field. The decay time constant was reduced from 25 s to 5 s by adding a small resistance (brass shims, approximately 50 nΩ) on the end of each lead. These resistors also helped to ensure that the current was shared more evenly among the return wires. This reduced the net torque and effects of the magnetic field of the return path to a negligible level.

The orientation of the sample was changed by rotating the sample cryostat relative to the background magnet. A pin in a series of circumferential holes at the top of the cryostat and the band brake mentioned above were used to hold the orientation. The zero angle was defined as the orientation with the magnetic field parallel to the wider side of the conductor. The zero position in the raw data was only approximate because of variation in how the sample was mounted in the holder.

Two experiments were conducted to test the apparatus and the effect. The first experiment was to measure I_c of a large (I_c 1200 A at 8 T) round wire as a function of angle from 0° to 360°. The measured critical currents were independent of angle within the experimental precision of ±1%. This result indicated that the apparatus had no artificial angular variation due to the applied magnetic field adding or subtracting from the magnetic field of the return leads.

The second experiment was a comparison of measurements made on a monolithic conductor and on a conductor composed of two of these monoliths soldered together along their length. This comparison was not ideal, but it allowed a direct comparison of aspect ratio effect and critical current. There were no indications of current-sharing problems in the I_c measurements.

Table 1. Physical Parameters of the Samples Measured.
Critical Current at 8 T for NbTi and 10 T for Nb_3Sn.

Sample number	Type	Conductor aspect	Filament aspect	I_c, A	ΔI_c, %	Cu/non Cu ratio
1	NbTi	round	~ 1.0	1215	< 1	2
2	NbTi	1.28	~ 1.11	114	5	1.8
3	NbTi	1.93	1.28 to 1.41	350	19 to 29	1.25
4	NbTi	2.0	1.15 to 1.17	700	19.5	2
5	NbTi	2.0	~ 1.24	600	17.5	5
6	NbTi	6.0	1.61 to 1.93	2350	42	5
7	Nb_3Sn	2.0	~ 1.92	42	15.5	1.63
8	Nb_3Sn	2.0	~ 3.15	1020	19	?

Within the experimental precision, I_c of the two-monolith conductor was
twice that of the single monolith and the aspect ratio effect was the same
percentage of I_c. These results suggested that the demagnetization factor
of the overall conductor did not have a significant effect.

DATA

    The general dependence of I_c on angle was similar for all samples
measured. It was more broad at $0°$ than at $90°$ and fell between $\sin^2\theta$ and
$\sin^4\theta$. Typical data are shown on Fig. 1 with $\sin^2\theta$ and $\sin^4\theta$ for reference.
The filaments were not perfectly aligned with the surface of the conductor;
some were tilted slightly on either side of alignment. This caused the
curve to be flat around $0°$ and is the most likely cause of the small peaks
observed in some of the samples (see Fig. 2) on either side of $0°$.

    The shape of I_c with angle scales approximately as a percentage of I_c
for the magnetic field range of 2 to 10 T (see Figs. 2, 3, and 4). Obviously,
the effect at zero magnetic field must be zero and should approach zero
continuously. In general, the effect at 2 T was a little lower percentage
than at higher magnetic fields. The lack of a strong field dependence
suggests that the fluxoid-core size and fluxoid spacing does not have a
large effect on the resulting pinning force.

    The aspect ratio effect in Nb_3Sn (see Fig. 4) is opposite that of
NbTi, but it is comparable in magnitude for similar conductor aspect
ratios. Two types of multifilamentary, bronze process Nb_3Sn conductors
were measured, one made using the conventional process and the other with
the jelly-roll process. Results were consistent between these two conductors.
A Nb_3Sn tape measured previously[3] had an aspect ratio effect in the same
direction as these multifilamentary Nb_3Sn conductors.

    The amount of asymmetric filament deformation, filament aspect ratio,
was determined from photographs of the wire cross sections. A large number
of filaments (in some cases all of the filaments) were averaged by summing
the ratio of width to thickness and then dividing by the number of filaments
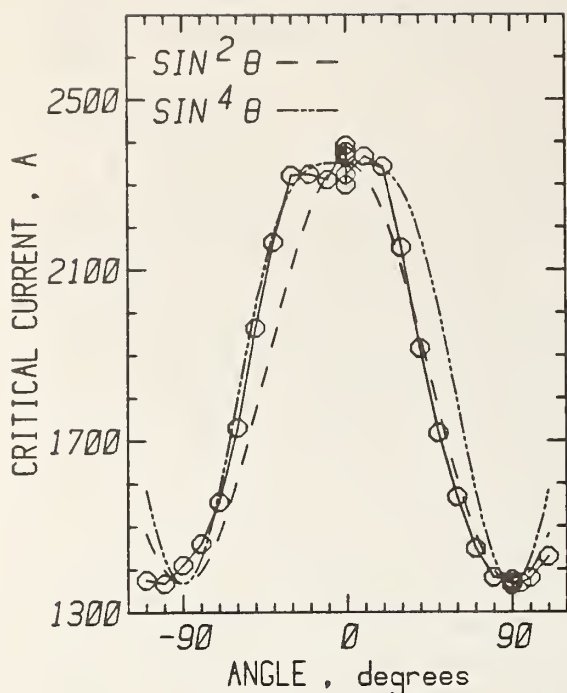to be averaged. These ratios are listed in Table 1.

Fig. 1. I_c versus angle for a NbTi conductor with an aspect ratio of 6, sample #6.
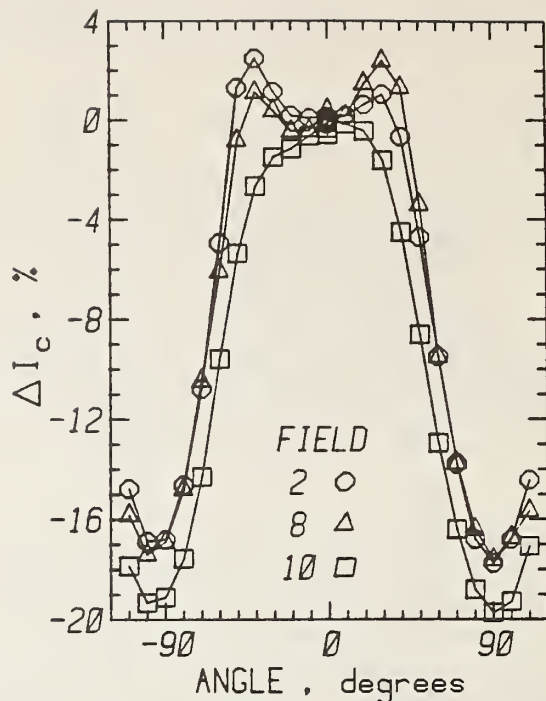

Fig. 2. Percentage change in I_c versus angle for NbTi sample #5.
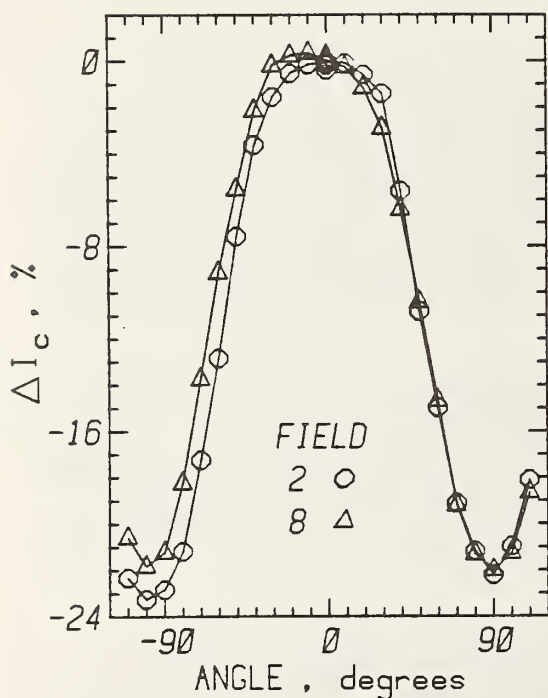
Fig. 3. Percentage change in I_c versus angle for NbTi sample #3.
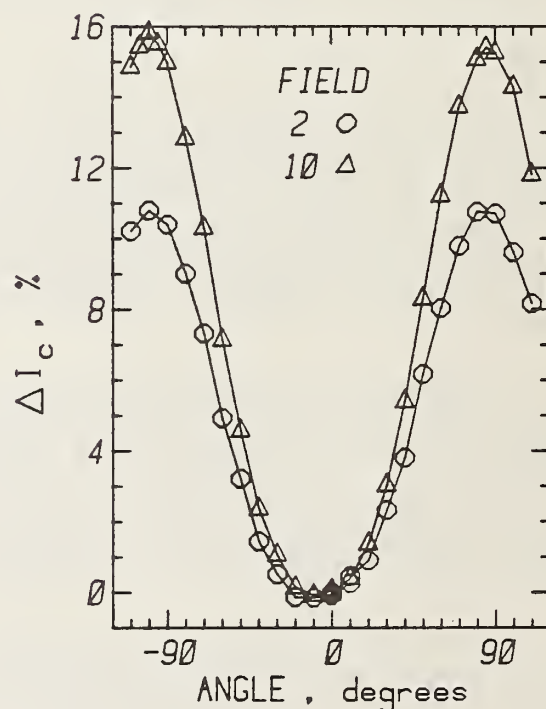
Fig. 4. Percentage change in I_c versus angle for Nb_3Sn sample #7.

Some filament aspect ratios of some wires varied by more than a factor of 2 for cross sections separated by less than a few centimeters along the length of the wire. Two such cross sections of the same wire are shown in Fig. 5. Further observation indicated that this variation might be occurring periodically along the conductor. As a result of this, another sample was prepared with a number of closely spaced voltage taps to look at short

46

range variation in I_c and aspect ratio effect. Figure 6 is a plot of I_c versus position along the wire using adjacent voltage taps separated by about 0.23 cm. Because of the close tap spacing (low voltage with $E_c = 0.2$ μV/cm) and I_c variation (quench current determined by the lowest I_c) a number of repeat determinations were made.

The variation in I_c was about 12% for the 0° data and 10% for the 90° data. The variation also looked periodic for both 0° and 90°. There was a high point for both the 0° and 90° data, starting from the left, approximately every third point. There was also a variation in the aspect ratio effect along the wire. Consider the third position: the 0° point was relatively low and the 90° point was relatively high, this resulted in a small aspect ratio effect. The situation was reversed for the fifth position, which results in a large aspect ratio effect and alternates along the wire. The aspect ratio effect varied from 19 to 29%.

The cause of this periodic variation in filament shape, I_c, and aspect ratio was most likely the combination of filament twist and hexagonal filament array.[4] Filament deformation was extreme when the flats of the hexagonal filament array were parallel to the minor dimension, where the filaments were on top of each other. A transverse view of the filaments etched from the matrix indicated that the wavelength of the extreme filament deformation was about 0.28 cm, which was about 1/6 of the twist length. The length of the flattened filament was about 0.1 cm. The fact that the tap separation was about the same as the deformation wavelength, apparently resulted in a beating of the two, forming a third artificial wavelength in the variation of I_c. The measured I_c values were consistent with a 0.28 cm wavelength but the actual amplitude of the variation may be larger. Measurements with a smaller tap separation, on the order of 0.05 cm, would have been very difficult because of the extremely low voltages.
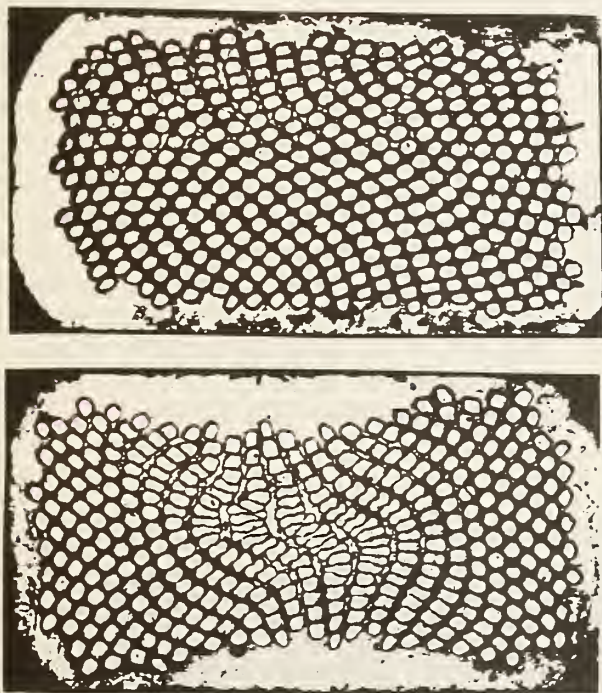

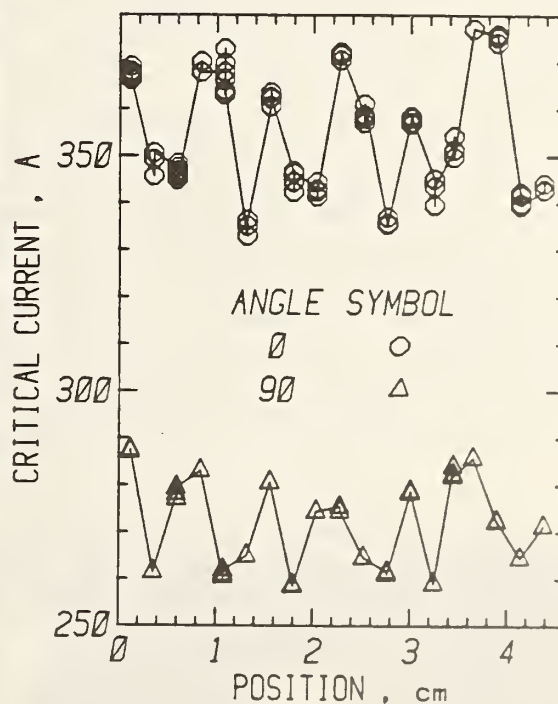Fig. 5. Photographs of two different cross sections of the same NbTi wire, sample #3.

Fig. 6. Variation of I_c versus position for 0° and 90° at 8 T and $E_c = 0.2$ μV/cm for sample #3.

47

The cross sections of other rectangular conductors were examined more closely considering this periodic filament deformation. All of the others measured showed some change in deformation as indicated by a change in the filament array. Two cross sections of the same wire are shown in Fig. 7. Notice the change in the shape of the center copper island and difference in filament deformation. Voltage tap and microscope studies did not reveal another case as extreme as Fig. 5, but there was always some variation. The physical parameter that may have been unique to the sample shown in Fig. 5 was the low copper to superconductor ratio 1.25/1.

Some measurements were made on a seven-strand NbTi cable, which had been compacted into a rectangular cross section. A photograph of the cable cross section is given in Fig. 8. A strand changes from almost round in the middle top position to deformed at the corner and side positions of the cable. Despite current sharing among the strands, V-I curves on short sections of individual strands gave some indication of the local I_c.

A number of voltage taps were placed along individual strands to measure I_c for different cable positions. Three regions of the cable were measured: an "overall" region encompassing two cable twist lengths of a strand, a "top" region encompassing only the portion of a strand on top of the cable, and a "side" region encompassing the corners and side portions. The shorthand notation for these three regions from here on will be: overall, top, and side. Voltage taps for the top and side measurements were placed on the top and bottom (wider faces) near the corner of the cable on a given strand. One of these voltage taps was used for both the top and side measurements. This placement caused most of the corner region to be included in the side measurement. Thus, all strand regions were included in either the top or the side measurements.

The cable I_c data had a combination of aspect ratio and self field effects. The self field of the conductor vectorially added to the applied magnetic field, which resulted in different magnetic fields for different angles and cable positions. The I_c of three regions of the cable versus angle are given in Fig. 9. The overall I_c, circles, had some structure approximately every 45° but the variation was less than 2%. Combining the aspect and self field effects, the top I_c as a function of angle should have been ordered in magnitude as follows; 180° > 0° > -90° and 90°. The side I_c should have been ordered in magnitude as follows; -90° > 90° > 180° and 0°. In fact, these experimental data and data on two other strands were consistent with this ordering. The only difference was a splitting of the lower critical currents. This was caused by a mixture of top and side characteristics due to the finite width of the transition from top to side. Notice that I_c for -90° top was greater than 90° top because I_c for -90° side was at a maximum. Also, I_c for 180° side was greater than 0° side because I_c for 180° top was at a maximum.
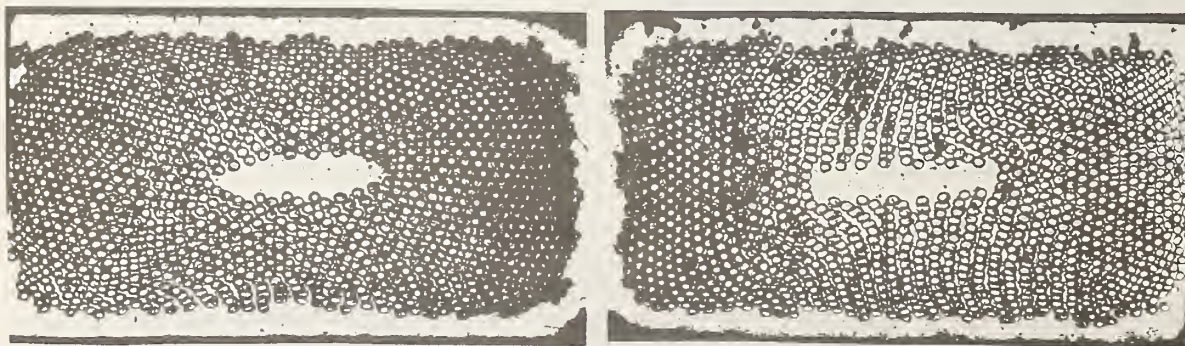

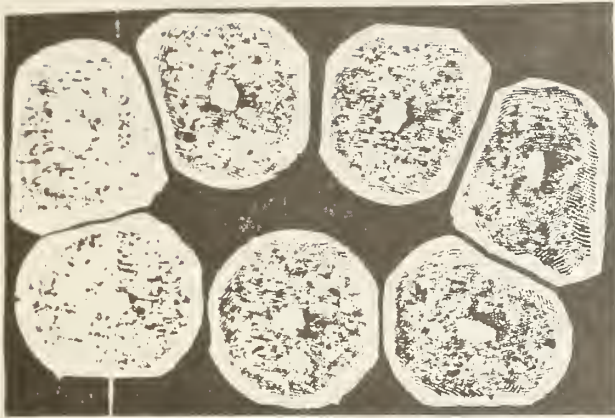Fig. 7. Photographs of two different cross sections of sample #5.

48

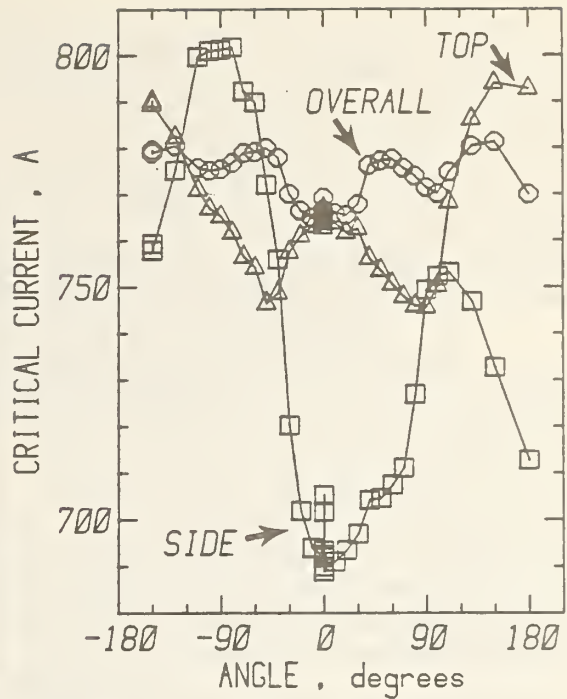Fig. 8. Photograph of the cross section of a NbTi cable.

Fig. 9. I_c versus angle for different regions of a NbTi cable, see Fig. 8.

The size of the aspect ratio and self field effects can be estimated with the assumption that the self field effect can be removed by averaging the critical currents taken 180° apart. Using this assumption at 8 T, the top has an aspect ratio effect of 8% and a self field effect of 3%. The side at 8 T has an aspect ratio effect of 14% and a self field effect of 6%. At 4 T, the aspect ratio and self field effects respectively are: top 6% and 5%; side 19% and 10%.

DISCUSSION

The most likely cause of the aspect ratio effect is the asymmetric deformation of the filaments and thus the orientation of the flux-pinning sites. If the magnetic fluxoid is more closely aligned with the pinning site, the pinning force will be larger than in the nonaligned orientation.[5] Extending to the whole conductor cross section, the total pinning force will be anisotropic. In the case of NbTi, the pinning sites (precipitates, dislocations, and impurities) have a preferred orientation parallel to the wider side of the filament (the wider side of the overall conductor) thus the higher critical current with the magnetic field in that orientation. For Nb_3Sn, the pinning sites (grain boundaries) have a preferred orientation perpendicular to the wider side of the filament, due to columnar grain growth; therefore, Nb_3Sn has the opposite orientation effect. Even though there is a mixture of equiaxial and columnar grain growth, the presence of some columnar grains apparently causes the total pinning force to be asymmetric.

The effect in Nb_3Sn is opposite that of NbTi, but it is comparable in magnitude for similar conductor aspect ratios. Due to the relative hardness, the Nb filaments in the bronze matrix (Nb_3Sn) is deformed more than the NbTi filaments in the copper matrix. However, as mentioned above, the mechanism is different for the two materials and the resulting effect on I_c is similar.

49

The lack of a strong field dependence of the percentage change in I_c with angle suggests that the fluxoid-core size and fluxoid spacing do not have a large effect on the resulting pinning force[6]. The samples measured in this study had a minimum amount of area reduction in going from a round to a rectangular cross section. However, for thin, highly deformed pinning sites, the change in fluxoid-core size with magnetic field could cause a strong field dependence of I_c with angle for NbTi. A sign reversal has been observed in rolled NbTi conductors[7] between low magnetic fields (I_c higher at 0°) and high magnetic fields (I_c higher at 90°).

In order to make these results more general, an empirical relationship between the size of the effect and some physical parameter was sought. With a predictive relationship, the size of the effect in more complex conductors, such as compacted cables, could be estimated. The aspect ratio of the filaments was the obvious choice. However, as shown above, there was too much variation for even a simple estimate. There might also be a dependence on the manufacturing technique. These data exemplify the magnitude and shape of the aspect ratio effect.

CONCLUSIONS

The aspect ratio has a significant effect on the critical current of rectangular monolithic and compacted cable NbTi and Nb_3Sn conductors. A 20% change in critical current with angle in a constant applied magnetic field is typical. The most likely cause of the aspect ratio effect is the asymmetric deformation of the filaments and thus the orientation of the flux-pinning sites. The effect in Nb_3Sn is opposite that of NbTi due to the different kinds of pinning sites in the two materials. Aspect ratio and self field effects can be observed in I_c measurements on a cable, which would account for some of the degradation of I_c from strand to cable. Large variations in filament deformation, critical current, and aspect ratio can be observed in rectangular conductors along the length of a wire.

ACKNOWLEDGMENTS

The authors extend their thanks to M. S. Allen for drafting and cryostat construction; F. R. Fickett for being an always available sounding board; J. W. Ekin for discussions of flux pinning; R. G. Benson for making sample holders; R. A. Shenko for preparing this paper; and to the rest of the Superconductors and Magnetic Materials Group.

REFERENCES

1. Standard Test Method for D-C Critical Current of Composite Superconductors, Annual Book of ASTM Standards, ASTM B714-82, Part 02.03, pp. 595-98, American Society for Testing and Materials, Philadelphia, Pennsylvania (1983).
2. S. L. Wipf, Los Alamos National Laboratory, Los Alamos, New Mexico, private communication.
3. L. F. Goodrich and F. R. Fickett, "Critical current measurements: a compendium of experimental results," Cryogenics 22: 222-241, 1982.
4. C. King, Intermagnetics General Corporation, Guilderland, New York, private communication.
5. A. M. Campbell and J. E. Evetts, "Flux vortices and transport currents in type II superconductors," Adv. Phys. 21: 199-429 (1972).
6. J. W. Ekin, "Critical currents in granular superconductors," Phys. Rev. B 12: 2676-2681 (1975).
7. M. Suenaga, Brookhaven National Lab., Upton, New York, private communication.

Quench detector circuit for superconductor testing

W. P. Dubé and L. F. Goodrich

Electromagnetic Technology Division, National Bureau of Standards, Boulder, Colorado 80303

A quench detector is a device that interrupts the flow of current through a superconductor in the event the superconductor reverts to the normal, resistive state. This new design has adjustable filtering and sensitivity. The input is well isolated from the output, eliminating any possible ground loop through the detector. It also has excellent noise immunity. A detector has operated with no false trips for more than two years, detecting hundreds of quenches.

INTRODUCTION

When testing superconducting wire with high current densities, it is usually necessary to interrupt sample current in the event of a quench.[1] A quench occurs when the sample leaves the superconducting state and begins a thermal runaway caused by resistive heating. Sample damage due to overheating may occur within a fraction of a second after the onset of a quench, depending on factors such as sample geometry, cooling, and thermal mass. In order to prevent such damage, an automatic device is necessary to detect the quench and reset the power supply to zero. The block diagram of a critical current measurement apparatus, shown in Fig. 1, illustrates a typical use of a quench detector in conjunction with other instruments in a critical current experiment.[2]

A good quench detector should have the following qualities: (1) Be capable of resetting the power supply rapidly enough to prevent sample damage. (2) Be able to detect both slow and rapid quenches. (3) Introduce no ground loops or extraneous signals into the system. (4) Be insensitive to noise and only reset the power supply in the event of an actual quench. (5) Be relatively simple, cheap, and easy to build.

I. CIRCUIT DESCRIPTION

Experiments have shown that all of the above qualities were incorporated in the design of the detector. The resistors are 5% tolerance, except where noted on the schematic, Fig 2. Low-noise, high slew-rate, FET-input operational amplifiers were used in the prototype, but lower quality devices would have sufficed.

The first stage of the device is a differential amplifier with a 20-kΩ input impedance and a gain of ten. The differential input tends to eliminate false tripping due to common-mode voltages. dc coupling was chosen to allow the detection of a gradual quench. The input isolation from ground is more than a gigaohm if a high-quality, high-isolation power supply or a battery power supply is used. If a medium-quality commercial power module is used, the low-voltage common or center tap should be tied to line ground to prevent common-mode voltages caused by capacitive coupling of the primary and secondary windings of the power transformer.

These common-mode voltages may appear on the input terminals if the low voltage center tap is not grounded. In this configuration, the input isolation would be reduced to about 50 kΩ to ground.

The second stage of the device is a variable, third-order, low-pass, active filter.[3] This stage enables the user to choose high noise rejection, fast reset speed, or a compromise between these two extremes. Roll-off frequency selection ranging from 10 Hz to 1 kHz is adequate for typical uses.

The third stage provides a variable gain from 0.1 to 200. The gain directly determines the minimum dc trip level. Reset speed is also a function of gain. Higher gain settings increase reset speed but tend to decrease noise rejection.

An arm/stand-by switch connects the third and fourth stages. This switch enables or disables the detector without causing the power supply to reset. Some current supplies produce a large transient when initially turned on. If the detector were not disabled during this transient, it might reset such a power supply whenever an attempt was made to turn on the supply.

The fourth and final stage of the detector is an opto-coupler that isolates the internal detector circuitry from any voltage appearing on the output terminals. This section has multiple purposes: first, it virtually eliminates any possibility of a ground loop through the detector; second, it prevents any noise, emanating from the controller or elsewhere, from entering the detector via the output terminals; and third, the diodes in the opto-isolators have a threshold voltage that provides a good transition between output logic states.

The output of the quench detector is connected to the reset input of the current supply controller. The controller reset input shown in Fig. 2 is typical, but other configurations may be used as long as the input/output isolation is not degraded. This degradation may occur if any part of the internal circuitry of the detector becomes electrically coupled with the controller circuitry.

It should be noted that it is best to use a separate set of sample voltage taps for the quench detector input. These taps should not be used for data acquisition. This reduces the possibility of one system interfering with the other. Ideally, the quench detector voltage taps should be placed at the extreme ends of the sample. In this way, a quench occurring in any portion of the sample will trigger the detector.
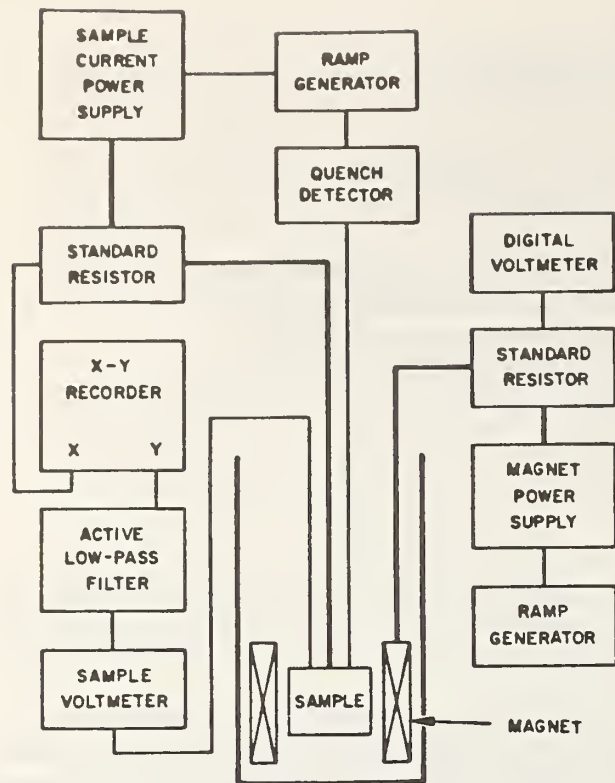
51

FIG. 1. Block diagram showing a typical use of a quench detector.

II. DISCUSSION

This section describes why a quench detector must be adjustable for different experimental conditions and how to go about determining the actual gain and filter settings.

Many factors must be considered in choosing the optimum quench detector gain and filter settings. The primary goal is to limit the temperature of the sample under test. The superconducting properties of the sample will be affected if the temperature is allowed to stay too high for too long. The difficulty arises in that there is no known way to calculate the minimum temperature (T_d) at which damage or change will occur. If the sample is subjected to mechanical stress, T_d can be suprisingly low, perhaps 77 K or lower. This mechanical stress can be caused by Lorentz force, differential thermal contraction, or deliberate loading. Under these conditions, sample damage is due to plastic deformation which causes a change in the superconducting properties of the sample. Since yield strength and creep rate are both strong functions of temperature, T_d is a strong function of mechanical stress.

Large nonlinearities in sample heat capacity, resistivity, normal-zone propagation velocity, heat transfer to the liquid-helium bath, etc. make rigorous mathematical analysis of the time-and-temperature-dependent sample voltage an arduous, if not impossible, task. This, in turn, makes calculation of the true optimum setting of the gain and filter imprac-
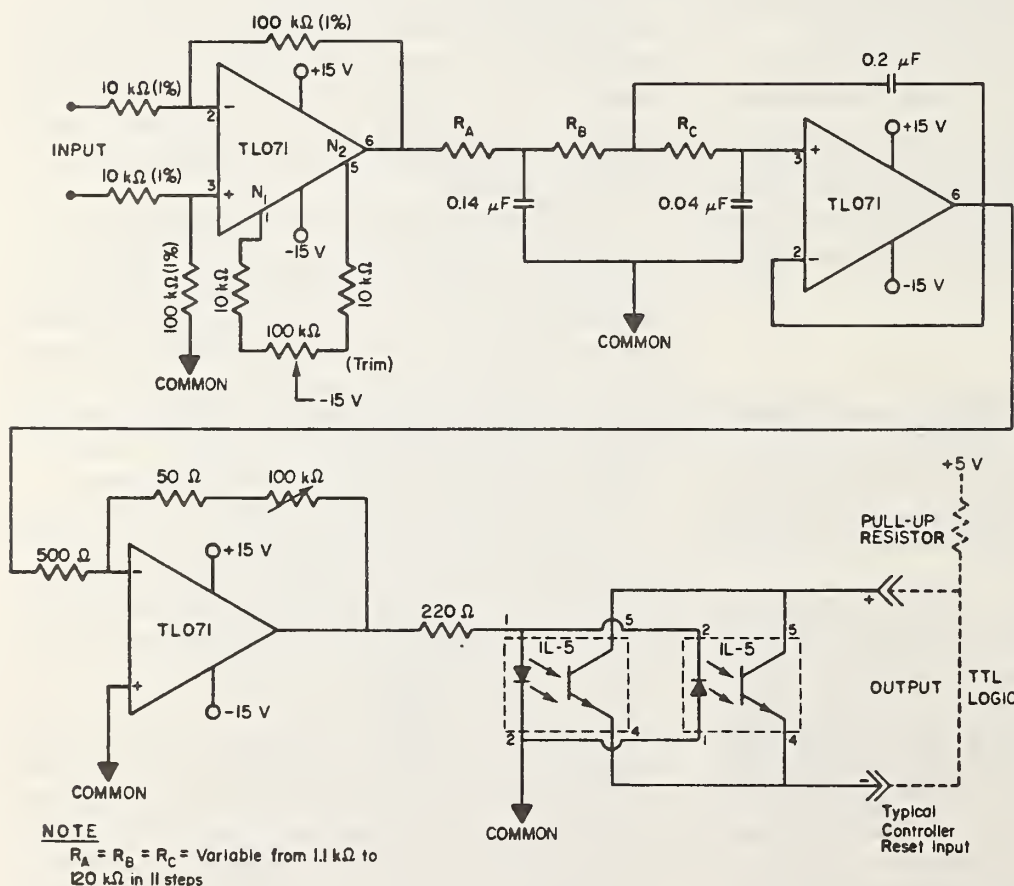

FIG. 2. Schematic diagram of the quench detector. The use of manufacturers' part numbers does not imply an endorsement by the National Bureau of Standards, nor does it imply that the devices identified are necessarily the best available for the purpose.

NOTE
$R_A = R_B = R_C =$ Variable from 1.1 kΩ to 120 kΩ in 11 steps

tical. The simplest and perhaps the most conservative approach to this problem is to estimate the low-temperature (4 K) normal-state resistance of the sample. The gain setting can be approximated as follows:

$$GAIN \cong 1.0/(RI)$$

using the estimated resistance R and test current I.

The filter setting is determined experimentally by starting at the highest (1 kHz) setting and attempting to energize the sample. The filter setting is then reduced as necessary to avoid false trip events. The distinction between true and false events can be made using an oscilloscope. If an actual quench has occurred, normal-state voltage appears along the sample before the current interruption and an inductive voltage, due to the rapid decrease in current, appears after the current interruption. If a quench has not occurred, only the voltage induced by the rapid decrease in current will be evident. If the filter setting derived by this method results in an excessively long time delay between quench event and current interruption, the filter setting selection process must be performed again at lower gain setting. The objective is to keep the sample temperature rise to a minimum, but this ideal must be balanced against the time lost due to false trip events.

The filter setting greatly affects the time delay between quench event and current shut down. With the filter section bypassed, and the sensitivity set to 5 mV, the elapsed time between the input of a 10-mV step and controller shut down is less than 30 μs. Using the same input and sensitivity settings, the delay varies from 0.38 ms at a filter setting of 1 kHz to 31 ms at a filter setting of 10 Hz. Time delay through the detector is a function of filter setting, gain setting, and input signal magnitude and shape. Time delays due to the power supply and the controller must be considered when estimating the total system time delay.

Experimental conditions determine the amount of time delay that may be tolerated. The following conditions, listed in descending order of importance, will allow an increase in the length of time that the sample may remain in the normal, resistive state without damage: (1) low sample current density; (2) low mechanical stress; (3) high sample heat capacity; (4) good thermal anchoring of the sample to a sample holder with high thermal diffusivity and heat capacity; and (5) sample and sample holder that are capable of good convective heat transfer to the surrounding liquid-helium bath.

This quench detector has prevented sample damage during many critical current and transient loss measurements. The detector appears to have all the qualities necessary for safe, reliable detection of quench and shut down of the sample power supply.

Because of the differential input, the high input impedance, and the good output isolation, no noticeable undesirable signals or ground loops were introduced into the system. Noise produced by nearby electrical equipment (drills, soldering guns, etc.), or ripple and SCR spikes produced by the sample current supply never caused false tripping when an appropriate filter setting was selected. Repeatable steady-state dc trip levels from 0.0006 to 0.500 V were possible because dc coupling was used throughout the detector.

ACKNOWLEDGMENT

[1]*Annual Book of ASTM Standards.* Standard Test Method for dc Critical Current of Composite Superconductors (American Society for Testing and Materials, Philadelphia, 1983), B714-82, Part 2.03, pp. 595–98.

[2]L. F. Goodrich and F. R. Fickett, *Cryogenics* 22, 225 (1982).

[3]A. B. Williams, *Active Filter Design* (Artech House, Dedham, MA, 1975).

53

PUBLICATIONS AND PRESENTATIONS

1. A. F. Clark and J. W. Ekin, "Defining Critical Current," IEEE Trans. Mag. MAG-13, 38-40 (1977).

2. R. L. Powell and A. F. Clark, "Definitions of Terms for Practical Super-conductors, 1. Fundamental States and Flux Phenomena," Cryogenics 17, 697-701 (1977).

3. R. L. Powell and A. F. Clark, "Definitions of Terms for Practical Super-conductors, 2. Critical Parameters," Cryogenics 18, 137-141 (1978).

4. J. W. Ekin, "Current Transfer in Multifilamentary Superconductors. I. Theory," J. Appl. Phys. 49, 3406-3409 (1978).

5. J. W. Ekin, A. F. Clark, and J. C. Ho, "Current Transfer in Multifila-mentary Superconductors. II. Experimental Results," J. Appl. Phys. 49, 3410-3412 (1978).

6. A. F. Clark, J. W. Ekin, R. Radebaugh, and D. T. Read, "The Development of Standards for Practical Superconductors," IEEE Trans. Mag. MAG-15, 224-227 (1979).

7. F. R. Fickett and A. F. Clark, "Development of Standards for Supercon-ductors, Annual Report FY 79," NBSIR 80-1629, National Bureau of Standards, Boulder, Colorado (Dec. 1979).

8. F. R. Fickett and A. F. Clark, "Standards for Superconductors," Prof. 1979 Mech. and Mag. Energy Storage Contractors' Review Meeting, Conf-790854, U.S. Dept. of Energy, Washington, DC (Dec. 1979).

9. D. T. Read, J. W. Ekin, R. L. Powell, and A. F. Clark, "Definitions of Terms for Practical Superconductors: 3. Fabrication, Stabilization, and Transient Losses," Cryogenics 19, 327-332 (1979).

10. F. R. Fickett and A. F. Clark, "Development of Standards for Supercon-ductors," Prof. 8th Int'l. Cryo. Eng. Conf. (ICEC8), IPC Science and Technology Press (1980) pp. 494-498.

11. F. R. Fickett and L. F. Goodrich, "NBD Superconductor Standardization Program," Prof. 1980 Superconducting MHD Magnet Design Conference A. M. Dawson, ed., (Report published by Bitter National Magnet Laboratory, MIT, Oct. 1981) p. 87-89.

12. F. R. Fickett, S. B. Kaplan, R. L. Powell, R. Radebaugh, and A. F. Clark, "Definitions of Terms for Practical Superconductors: 4. Josephson Phenomena," Cryogenics 20, 319-325 (1980).

13. G. Fujii, J. W. Ekin, R. Radebaugh, and A. F. Clark, "Effect of Thermal Contraction of Sample Holder Material on Critical Current," Adv. Cryog. Eng. Vol. 26, Plenum Press, New York (1980) p. 589-598.

14. G. Fujii, "Present Practices in Japan for the Measurement and Definition of Various Superconducting Parameters," Tech. Report ISSP Univ. of Tokyo, Ser. A, No. 1063 (July 1980).

15. G. Fujii, J. W. Ekin, R. Radebaugh, and A. F. Clark, "Effect of Thermal Contraction of Sample-Holder Material on Critical Current," Tech. Report ISSP Univ. of Tokyo, Ser. A, No. 1074 (Aug. 1980).

16. A. F. Clark, "Development of Standards for Practical Superconductors," Proc. Superconductivity Technical Exchange Meeting, IAPG, PIC-ELE-SC 209/1 (1980), p. 103 (presentation only).

17. L. F. Goodrich and J. W. Ekin, "Lap Joint Resistance and Intrinsic Critical Current Measurements on a NbTi Superconducting Wire," Proc. 1980 Applied Superconductivity Conference, IEEE Trans. Mag. MAG-17, 69-72 (1981).

18. R. Radebaugh, G. Fujii, D. T. Read, and A. F. Clark, "A Standards Program for ac Losses in Superconductors," Proc. IVth Int'l. Congress on Refrigeration (1980), Comm. A 1/2-10 (1980)., pp. 1-4.

19. G. Fujii, "Present Practices in Japan for the Measurement and Definition of Various Superconducting Parameters," Cryogenics 21, 21-38 (1981).

20. H. R. Segal, Z. J. J. Stekley, and T. A. DeWinter, "Development of Critical Current Measurement Standards," Proc. 1980 Applied Superconductivity Conference, IEEE Trans. Mag. MAG-17, 73-76 (1981).

21. G. Fujii, M. A. Ranney, and A. F. Clark, "Thermal Expansion of Nb_3Sn and V_3Ga Multifilamentary Superconducting Cables, Fiberglass-Epoxy and Cotton-Phenolic Composite Materials," Jap. J. Appl. Phys. 20, L267-L270 (1981).

22. L. F. Goodrich, J. W. Ekin, and F. R. Fickett, "Effect of Twist Pitch on Short-Sample V-I Characteristics of Multifilamentary Superconductors," Adv. Cryog. Eng. - Materials, Vol. 28, Plenum Press, New York (1981), p. 571-580.

23. A. F. Clark, G. Fujii, and M. A. Ranney, "The Thermal Expansion of Several Materials for Superconducting Magnets," IEEE Trans. Mag. MAG-17, 2316-2319 (1981).

24. F. R. Fickett, L. F. Goodrich, and A. F. Clark, "Development of Standards for Superconductors: Annual Report FY 80," NBSIR 80-1642, National Bureau of Standards, Boulder, Colorado (Dec. 1980).

25. L. F. Goodrich and F. R. Fickett, "Critical Current Measurements: A Compendium of Experimental Results," Cryogenics 22, 225-241 (1982).

26. A. F. Clark, L. F. Goodrich, F. R. Fickett, and J. V. Minervini, "Development of Standards for Superconductors, Interim Report Oct. 80 to Jan. 82," NBSIR 82-1678, National Bureau of Standards, Boulder, Colorado (July 1982).

27. Standard Definitions of Terms Relating to Superconductors, Annual Book of ASTM Standards, ASTM B713-82, Part 2.03, pp. 591-594, American Society for Testing and Materials, Philadelphia, PA (1983).

28. Standard Test Method for D-C Critical Current of Composite Superconductors, Annual Book of ASTM Standards, ASTM B714-82, Part 2.03, pp. 595-98, American Society for Testing and Materials, Philadelphia, PA (1983).

29. L. F. Goodrich, "The Effect of Field Orientation on Current Transfer in Multifilamentary Superconductors," IEEE Trans. Mag. <u>MAG-19</u>, 244-247 (1983).

30. L. F. Goodrich, E. S. Pittman, and A. F. Clark, "Critical Current Measurements on Standard Reference Material," <u>Adv. Cryo. Eng.</u> - <u>Materials</u>, <u>Vol. 30</u>, Plenum Press, New York (1984), pp. 953-960.

31. A. F. Clark, L. F. Goodrich, and F. R. Fickett, "Experience in Standardizing Superconductor Measurements," J. Physique <u>45(C1)</u>, 379-382 (1984).

32. L. F. Goodrich, D. F. Vecchia, E. S. Pittman, J. W. Ekin, and A. F. Clark, "Critical Current Measurements on an NbTi Superconducting Wire Standard Reference Material," NBS Special Publication 260-91 (1984).

33. A. F. Clark and L. F. Goodrich, "Characterization of a Standard Reference Superconductor for Critical Current and a Summary of Other Standard Research at NBS," <u>Proc. Tenth International Cryogenic Engineering Conference</u> (1984), Butterworth & Co. Ltd., p. 433-437 (1984).

34. L. F. Goodrich, J. V. Minervini, A. F. Clark, F. R. Fickett, J. W. Ekin, and E. S. Pittman, "Development of Standards for Superconductors, Interim Report Jan. 82 to Dec. 83," NBSIR 85-3027, National Bureau of Standards, Boulder, Colorado (Jan. 1985).

35. L. F. Goodrich, W. P. Dube, E. S. Pittman, and A. F. Clark, "The Effect of Aspect Ratio on Critical Current in Multifilamentary Superconductors," <u>Adv. Cryo. Eng.</u> - <u>Materials</u>, <u>Vol. 32</u>, Plenum Press, New York (1986).

36. W. P. Dube and L. F. Goodrich, "Quench Detector Circuit for Superconductor Testing," <u>Rev. Sci. Instrum.</u>, <u>57</u>, 680-682 (1986).

U.S. DEPT. OF COMM. **BIBLIOGRAPHIC DATA** SHEET (See instructions)	1. PUBLICATION OR REPORT NO. NBSIR 87-3066	2. Performing Organ. Report No.	3. Publication Date April 1987

4. TITLE AND SUBTITLE

DEVELOPMENT OF STANDARDS FOR SUPERCONDUCTORS
Interim Report
January - December 1985

5. AUTHOR(S)

L.F. Goodrich, S.L. Bray, W.P. Dube, E.S. Pittman, A.F. Clark

6. PERFORMING ORGANIZATION (If joint or other than NBS, see instructions) **NATIONAL BUREAU OF STANDARDS** **DEPARTMENT OF COMMERCE** **WASHINGTON, D.C. 20234**	7. Contract/Grant No.
	8. Type of Report & Period Covered

9. SPONSORING ORGANIZATION NAME AND COMPLETE ADDRESS (Street, City, State, ZIP)

10. SUPPLEMENTARY NOTES

☐ Document describes a computer program; SF-185, FIPS Software Summary, is attached.

11. ABSTRACT (A 200-word or less factual summary of most significant information. If document includes a significant bibliography or literature survey, mention it here)

A cooperative program with the Department of Energy, the National Bureau of Standards, and private industry is in progress to develop standard measurement practices for use in large scale applications of superconductivity. The goal is the adoption of voluntary standards for the critical parameters and other characterizations of practical superconductors. Progress for the period January through December 1985 is reported. The major effort was the measurement of large conductor critical current. Other work reported here includes stability and a discussion of possible future Standard Reference Materials.

12. KEY WORDS (Six to twelve entries; alphabetical order; capitalize only proper names; and separate key words by semicolons)

angle; aspect ratio; cable; critical current; critical parameters; measurement; standards; superconductor

13. AVAILABILITY ☒ Unlimited ☐ For Official Distribution. Do Not Release to NTIS ☐ Order From Superintendent of Documents, U.S. Government Printing Office, Washington, D.C. 20402. ☒ Order From National Technical Information Service (NTIS), Springfield, VA. 22161	14. NO. OF PRINTED PAGES 64
	15. Price